



## Mutations disrupting neuritogenesis genes confer risk for cerebral palsy

Item Type	Article
Authors	Jin, Sheng Chih; Lewis, Sara A; Bakhtiari, Somayeh; Zeng, Xue; Sierant, Michael C; Shetty, Sheetal; Nordlie, Sandra M; Elie, Aureliane; Corbett, Mark A; Norton, Bethany Y; van Eyk, Clare L; Haider, Shozeb; Guida, Brandon S; Magee, Helen; Liu, James; Pastore, Stephen; Vincent, John B; Brunstrom-Hernandez, Janice; Papavasileiou, Antigone; Fahey, Michael C; Berry, Jesia G; Harper, Kelly; Zhou, Chongchen; Zhang, Junhui; Li, Boyang; Heim, Jennifer; Webber, Dani L; Frank, Mahalia S B; Xia, Lei; Xu, Yiran; Zhu, Dengna; Zhang, Bohao; Sheth, Amar H; Knight, James R; Castaldi, Christopher; Tikhonova, Irina R; López-Giráldez, Francesc; Keren, Boris; Whalen, Sandra; Buratti, Julien; Doummar, Diane; Cho, Megan; Retterer, Kyle; Millan, Francisca; Wang, Yangong; Waugh, Jeff L; Rodan, Lance; Cohen, Julie S; Fatemi, Ali; Lin, Angela E; Phillips, John P; Feyma, Timothy; MacLennan, Suzanna C; Vaughan, Spencer; Crompton, Kylie E; Reid, Susan M; Reddihough, Dinah S; Shang, Qing; Gao, Chao; Novak, Iona; Badawi, Nadia; Wilson, Yana A; McIntyre, Sarah J; Mane, Shrikant M; Wang, Xiaoyang; Amor, David J; Zarnescu, Daniela C; Lu, Qiongshi; Xing, Qinghe; Zhu, Changlian; Bilguvar, Kaya; Padilla-Lopez, Sergio; Lifton, Richard P; Gecz, Jozef; MacLennan, Alastair H; Kruer, Michael C
Citation	Jin, S.C., Lewis, S.A., Bakhtiari, S. et al. Mutations disrupting neuritogenesis genes confer risk for cerebral palsy. <i>Nat Genet</i> 52, 1046–1056 (2020). <a href="https://doi.org/10.1038/s41588-020-0695-1">https://doi.org/10.1038/s41588-020-0695-1</a>
DOI	<a href="https://doi.org/10.1038/s41588-020-0695-1">10.1038/s41588-020-0695-1</a>
Publisher	NATURE RESEARCH
Journal	NATURE GENETICS

Rights	Copyright © 2020, The Author(s), under exclusive licence to Springer Nature America, Inc.
Download date	28/08/2023 20:22:02
Item License	<a href="http://rightsstatements.org/vocab/InC/1.0/">http://rightsstatements.org/vocab/InC/1.0/</a>
Version	Final accepted manuscript
Link to Item	<a href="http://hdl.handle.net/10150/648094">http://hdl.handle.net/10150/648094</a>

# Mutations disrupting neuritogenesis genes confer risk for cerebral palsy

Sheng Chih Jin<sup>1,2,3,32</sup>, Sara A. Lewis<sup>4,5,32</sup>, Somayeh Bakhtiari<sup>4,5,32</sup>, Xue Zeng<sup>1,2,32</sup>, Michael C. Sierant<sup>1,2</sup>, Sheetal Shetty<sup>4,5</sup>, Sandra M. Nordlie<sup>4,5</sup>, Aureliane Elie<sup>4,5</sup>, Mark A. Corbett<sup>6</sup>, Bethany Y. Norton<sup>4,5</sup>, Clare L. van Eyk<sup>6</sup>, Shozeb Haider<sup>7</sup>, Brandon S. Guida<sup>4,5</sup>, Helen Magee<sup>4,5</sup>, James Liu<sup>4,5</sup>, Stephen Pastore<sup>8</sup>, John B. Vincent<sup>8</sup>, Janice Brunstrom-Hernandez<sup>9</sup>, Antigone Papavasileiou<sup>10</sup>, Michael C. Fahey<sup>11</sup>, Jesia G. Berry<sup>6</sup>, Kelly Harper<sup>6</sup>, Chongchen Zhou<sup>12</sup>, Junhui Zhang<sup>1</sup>, Boyang Li<sup>13</sup>, Jennifer Heim<sup>4</sup>, Dani L. Webber<sup>6</sup>, Mahalia S. B. Frank<sup>6</sup>, Lei Xia<sup>14</sup>, Yiran Xu<sup>14</sup>, Dengna Zhu<sup>14</sup>, Bohao Zhang<sup>14</sup>, Amar H. Sheth<sup>1</sup>, James R. Knight<sup>15</sup>, Christopher Castaldi<sup>15</sup>, Irina R. Tikhonova<sup>15</sup>, Francesc López-Giráldez<sup>15</sup>, Boris Keren<sup>16</sup>, Sandra Whalen<sup>16</sup>, Julien Buratti<sup>16</sup>, Diane Doummar<sup>16</sup>, Megan Cho<sup>17</sup>, Kyle Retterer<sup>17</sup>, Francisca Millan<sup>17</sup>, Yangong Wang<sup>18</sup>, Jeff L. Waugh<sup>19</sup>, Lance Rodan<sup>20</sup>, Julie S. Cohen<sup>21</sup>, Ali Fatemi<sup>21</sup>, Angela E. Lin<sup>22</sup>, John P. Phillips<sup>23</sup>, Timothy Feyma<sup>24</sup>, Suzanna C. MacLennan<sup>25</sup>, Spencer Vaughan<sup>26</sup>, Kylie E. Crompton<sup>27</sup>, Susan M. Reid<sup>27</sup>, Dinah S. Reddihough<sup>27</sup>, Qing Shang<sup>12</sup>, Chao Gao<sup>28</sup>, Iona Novak<sup>29</sup>, Nadia Badawi<sup>29</sup>, Yana A. Wilson<sup>29</sup>, Sarah J. McIntyre<sup>29</sup>, Shrikant M. Mane<sup>15</sup>, Xiaoyang Wang<sup>14,30</sup>, David J. Amor<sup>27</sup>, Daniela C. Zarnescu<sup>26</sup>, Qiongshi Lu<sup>31</sup>, Qinghe Xing<sup>18,33</sup>, Changlian Zhu<sup>14,30,33</sup>, Kaya Bilguvar<sup>1,15,33</sup>, Sergio Padilla-Lopez<sup>4,5,33</sup>, Richard P. Lifton<sup>1,2,33</sup>, Jozef Gecz<sup>6,33</sup>, Alastair H. MacLennan<sup>6,33</sup>, and Michael C. Kruer<sup>4,5,33\*</sup>

<sup>1</sup>Department of Genetics, Yale University School of Medicine, New Haven, CT, USA.

<sup>2</sup>Laboratory of Human Genetics and Genomics, Rockefeller University, New York, NY, USA.

<sup>3</sup>Department of Genetics, Washington University School of Medicine, St. Louis, MO, USA.

<sup>4</sup>Pediatric Movement Disorders Program, Division of Pediatric Neurology, Barrow Neurological Institute, Phoenix Children's Hospital, Phoenix, AZ, USA.

<sup>5</sup>Departments of Child Health, Neurology, Cellular & Molecular Medicine and Program in Genetics, University of Arizona College of Medicine, Phoenix, AZ, USA.

<sup>6</sup>Robinson Research Institute, The University of Adelaide, Adelaide, South Australia, Australia.

<sup>7</sup>Department of Pharmaceutical and Biological Chemistry, UCL School of Pharmacy, London, UK.

<sup>8</sup>Molecular Brain Sciences, Campbell Family Mental Health Research Institute, Centre for Addiction and Mental Health, Toronto, ON, Canada.

<sup>9</sup>One CP Place, Plano, TX, USA.

<sup>10</sup>Division of Paediatric Neurology, Iaso Children's Hospital, Athens, Greece.

<sup>11</sup>Department of Pediatrics, Monash University, Melbourne, Victoria, Australia.

<sup>12</sup>Henan Key Laboratory of Child Genetics & Metabolism, Rehabilitation Department, Children's Hospital of Zhengzhou University, Zhengzhou, China.

<sup>13</sup>Department of Biostatistics, Yale School of Public Health, New Haven, CT, USA.

<sup>14</sup>Henan Key Laboratory of Child Brain Injury, Third Affiliated Hospital of Zhengzhou University, Zhengzhou, China.

<sup>15</sup>Yale Center for Genome Analysis, Yale University, New Haven, CT, USA.

48 <sup>16</sup>Département de Génétique, Centre de Référence Déficiences Intellectuelles de  
49 Causes Rares, Groupe Hospitalier Pitié Salpêtrière et GHUEP Hôpital Trousseau,  
50 Sorbonne Université, GRC “Déficience Intellectuelle et Autisme”, Paris, France.  
51 <sup>17</sup>GeneDx, Gaithersburg, MD, USA.  
52 <sup>18</sup>Institute of Biomedical Science and Children's Hospital, and Key Laboratory of  
53 Reproduction Regulation of the National Population and Family Planning Commission  
54 (NPFPC), Shanghai Institute of Planned Parenthood Research (SIPPR), IRD, Fudan  
55 University, Shanghai, China.  
56 <sup>19</sup>Departments of Pediatrics & Neurology, University of Texas Southwestern and  
57 Children's Medical Center of Dallas, Dallas, TX, USA.  
58 <sup>20</sup>Departments of Genetics & Genomics and Neurology, Boston Children's Hospital,  
59 Boston, MA, USA.  
60 <sup>21</sup>Division of Neurogenetics and Hugo W. Moser Research Institute, Kennedy Krieger  
61 Institute, Baltimore, MD, USA.  
62 <sup>22</sup>Medical Genetics, Department of Pediatrics, MassGeneral Hospital for Children,  
63 Boston, MA, USA.  
64 <sup>23</sup>Departments of Pediatrics and Neurology, University of New Mexico, Albuquerque,  
65 NM, USA.  
66 <sup>24</sup>Division of Pediatric Neurology, Gillette Children's Hospital, St. Paul, Minnesota, USA.  
67 <sup>25</sup>Department of Paediatric Neurology, Women's & Children's Hospital, Adelaide, South  
68 Australia, Australia.  
69 <sup>26</sup>Departments of Molecular & Cellular Biology and Neuroscience, University of Arizona,  
70 Tucson, AZ, USA.  
71 <sup>27</sup>Murdoch Children's Research Institute and University of Melbourne Department of  
72 Paediatrics, Royal Children's Hospital, Melbourne, Victoria, Australia.  
73 <sup>28</sup>Rehabilitation Department, Children's Hospital of Zhengzhou University/Henan  
74 Children's Hospital, Zhengzhou, China.  
75 <sup>29</sup>Cerebral Palsy Alliance Research Institute, University of Sydney, Sydney, NSW,  
76 Australia.  
77 <sup>30</sup>Institute of Neuroscience and Physiology, Sahlgrenska Academy, Gothenburg  
78 University, Gothenburg, Sweden.  
79 <sup>31</sup>Department of Biostatistics & Medical Informatics, University of Wisconsin-Madison,  
80 Madison, WI, USA.  
81 <sup>32</sup>These authors contributed equally to this work.  
82 <sup>33</sup>These authors jointly directed this project.  
83 \*e-mail: [kruerm@email.arizona.edu](mailto:kruerm@email.arizona.edu)

84  
85  
86  
87  
88

89 **In addition to commonly associated environmental factors, genomic factors may**  
90 **cause cerebral palsy (CP). We performed whole exome sequencing in 250 parent-**  
91 **offspring trios, and observed enrichment of damaging *de novo* mutations (DNMs)**  
92 **in CP cases. Eight genes had multiple damaging DNMs; of these, two (*TUBA1A***  
93 **and *CTNNB1*) met genome-wide significance. We identified two novel monogenic**  
94 **etiologies, *FBXO31* and *RHOB*, and showed the *RHOB* mutation enhances active-**  
95 **state Rho effector binding while the *FBXO31* mutation diminishes cyclin D levels.**  
96 **Candidate CP risk genes overlapped with neurodevelopmental disorder genes.**  
97 **Network analyses identified enrichment of Rho GTPase, extracellular matrix, focal**  
98 **adhesion, and cytoskeleton pathways. CP risk genes in enriched pathways were**  
99 **shown to regulate neuromotor function in a *Drosophila* reverse genetics screen.**  
100 **We estimate that 14% of cases could be attributed to an excess of damaging *de***  
101 ***novo* or recessive variants. These findings provide evidence for genetically**  
102 **mediated dysregulation of early neuronal connectivity in CP.**

103  
104  
105 Cerebral palsy (CP) is the cardinal neurodevelopmental disorder impacting motor  
106 function, affecting ~2-3 per 1,000 children worldwide<sup>1,2</sup>. Movement disorder (spasticity,  
107 dystonia, choreoathetosis, and/or ataxia) onset occurs within the first few years of life as  
108 a manifestation of disrupted brain development<sup>3</sup>. Historically, although Little and Osler<sup>4</sup>  
109 considered CP to occur largely as a result of perinatal anoxia, Freud disputed this  
110 claim<sup>5</sup>. To this day, debate about the origin of CP continues, particularly in individual  
111 cases, with widespread medical and legal implications<sup>6,7</sup>.

112 Analogous to other neurodevelopmental disorders (NDD) such as autism  
113 spectrum disorders (ASD) and intellectual disability (ID), no single causative factor has  
114 been implicated in CP, although several environmental factors, including prematurity,  
115 infection, hypoxia-ischemia, and pre- and perinatal stroke, are major contributors to CP  
116 risk<sup>8</sup>. However, as many as ~40% of CP cases may not have a readily identifiable  
117 etiology<sup>9</sup>, defined as cryptogenic or idiopathic CP<sup>10</sup>. Registry-based data has shown that  
118 21-40% of CP cases have an associated congenital anomaly, implicating genomic  
119 alterations in many of these cases<sup>11</sup>. A heritability of 40% has been estimated in CP<sup>12</sup>,  
120 supported by probabilistic modeling of CP etiology in a western Swedish cohort<sup>13</sup>,  
121 comparable to the heritability of 38-58% estimated for ASD<sup>14,15</sup>.

122 To date, five studies have analyzed genomic copy number variations (CNVs) in  
123 CP cases<sup>10,16-19</sup>, identifying predicted deleterious CNVs in 10-31% of cases. Three prior  
124 whole exome sequencing (WES) studies have been performed in CP cases<sup>20-22</sup>. The  
125 largest study to date reported putatively deleterious variants in ~14% of 98 parent-  
126 offspring trios with unselected forms of CP<sup>22</sup>. These studies indicate potentially  
127 important genetic risks in CP, but insufficient availability of controls limited the statistical  
128 inferences that could be made, and functional validation of novel candidate gene  
129 variants was not performed. We sought to address these limitations in the current study.

## 130 131 **RESULTS**

132  
133 **CP cohort characteristics and WES.** We performed WES of 250 CP trios, including 91  
134 previously reported<sup>22</sup> and 159 ascertained from centers in the United States, China, and  
135 Australia after written informed consent was obtained according to local ethical

136 requirements (**Methods**). Cases were diagnosed by clinical specialists using  
137 international consensus criteria<sup>23</sup> (**Supplementary Table 1** and **Supplementary Data**  
138 **Set 1**); CP was thus defined as a non-progressive developmental disorder of movement  
139 and/or posture impairing motor function. Cases experienced symptom onset by age two.  
140 This operational definition thus excluded progressive neurological disorders such as  
141 neurodegenerative diseases. No cases had known chromosomal anomalies or  
142 aneuploidies, clinically or molecularly diagnosed syndromes (i.e. Rett syndrome,  
143 Angelman syndrome, etc.), pathogenic microdeletion or microduplication syndromes,  
144 mitochondrial disorders, or traumatic brain injuries.

145 Detailed patient phenotypes are available in the **Supplementary Note**.  
146 Representative neuroimaging findings are presented in **Extended Data Figure 1**, and  
147 videos highlighting movement disorder phenotypes in representative individuals can be  
148 found in **Supplementary Videos** (43 videos available via  
149 <https://figshare.com/s/a4f914ab77958ab3e4b6>) and in **Supplementary Photos**  
150 (<https://figshare.com/s/0f200402e51de5875390>). Within our 250 family cohort, 157 trios  
151 (62.8%) were classified as idiopathic (no known cause), 84 cases (33.6%) had a known  
152 environmental insult associated with CP (including prematurity defined as < 32 weeks  
153 gestation, perinatal hypoxia-ischemia (as defined by treating clinicians),  
154 ischemic/hemorrhagic stroke, and/or infection), and the remaining 9 trios (3.6%) were  
155 not able to be assigned to either category (“unclassified”) (**Supplementary Table 1**).

156 WES was performed as previously described<sup>24</sup> (see **Supplementary Table 2** for  
157 exome metrics). Control trios consisting of 1,789 unaffected siblings of autism cases  
158 and their unaffected parents from the Simons Simplex Collection were analyzed in  
159 parallel<sup>25</sup>. BWA-MEM was used to align the sequencing reads, and GATK ‘Best  
160 Practices’ was used to call variants<sup>26,27</sup>. MetaSVM<sup>28</sup> and Combined Annotation  
161 Dependent Depletion (CADD v1.3)<sup>29</sup> algorithms were used to predict deleteriousness of  
162 missense variants (“D-Mis”, defined as MetaSVM-deleterious or CADD  $\geq 20$ ). Inferred  
163 loss of function (LoF) variants consist of stop-gain, stop-loss, frameshift  
164 insertions/deletions, canonical splice site, and start-loss. LoF and D-Mis mutations were  
165 considered “damaging”. *De novo* mutations (DNMs) were called by the TrioDeNovo  
166 program<sup>30</sup>. Sanger sequencing was conducted to validate mutations in genes of  
167 interest.

168  
169 **Damaging DNMs are significantly enriched in the CP cohort.** We began by  
170 assessing the contribution of DNMs to CP at a cohort level. The number of observed  
171 DNMs in cases and controls closely approximates the Poisson distribution (**Extended**  
172 **Data Fig. 2**), indicating that DNMs are independent probabilistic events. We found an  
173 enrichment of damaging DNMs in CP cases, which became more apparent when  
174 focusing the analysis on genes intolerant to LoF variation (pLI score  $\geq 0.9$  in gnomAD  
175 v2.1.1<sup>31</sup>) (enrichment = 1.78;  $P = 1.2 \times 10^{-5}$  for damaging DNMs; **Table 1**). No  
176 significant enrichment of any mutation category was found in controls (**Table 1**). When  
177 we considered the ascertainment differential (observed number of damaging DNMs vs.  
178 expected number of damaging DNMs, divided by the number of trios in the cohort),  
179 11.9% of CP cases in our cohort could be attributed to an excess of damaging DNMs.  
180 When stratifying cases by CP subtype, we found greater enrichment of damaging DNMs  
181 in idiopathic (enrichment = 1.98;  $P = 2.1 \times 10^{-5}$ ) compared to environmental cases

182 (enrichment = 1.28;  $P = 0.19$ ; **Supplementary Table 3**), suggesting that idiopathic  
183 cases harbor a higher burden of damaging DNMs.

184  
185 **Recurrent damaging DNMs implicate both known and novel CP genes.** We next  
186 considered individual genes recurrently implicated in our CP cohort via a *de novo*  
187 mechanism (**Supplementary Data Set 2**). We identified eight genes harboring  $\geq 2$   
188 damaging DNMs, with *TUBA1A* ( $P = 4.8 \times 10^{-8}$ ) and *CTNNB1* ( $P = 9.8 \times 10^{-10}$ )  
189 surpassing Bonferroni correction cutoffs for genome-wide significance (**Table 2** and  
190 **Supplementary Table 4**). The gene-level enrichment of protein-damaging DNMs in  
191 these genes we observed strongly implicates these genes as *bona fide* CP-associated  
192 genes (**Supplementary Table 5**). Among these eight genes, *ATL1*, *CTNNB1*, *SPAST*,  
193 and *TUBA1A* have previously been associated with human CP phenotypes<sup>20,22,32</sup>. We  
194 also identified identical but independently arising damaging DNMs in two genes, *RHOB*  
195 and *FBXO31*.

196  
197 **Identical gain-of-function DNMs in *RHOB* and *FBXO31*.** *RHOB*, encoding a Rho  
198 GTPase, harbored two identical DNMs (p.Ser73Phe; **Fig. 1a** and **Supplementary**  
199 **Table 4**) in two unrelated spastic-dystonic CP cases, representing an unlikely chance  
200 event ( $P = 1.6 \times 10^{-3}$ ) (**Supplementary Note**). Ser73 is predicted to be phosphorylated  
201 (0.997 by NetPhos 3.1)<sup>33</sup> and located in a conserved position in the Switch II domain,  
202 where Rho protein kinases associate with Rho- and Rac-related proteins (**Fig. 1b**).  
203 Comparing structural models of *RHOB* wild-type and p.Ser73Phe suggests an alteration  
204 of both the shape of the binding site and the surface charge of the protein (**Fig. 1b**).  
205 Both patients have a remarkably concordant phenotype, including hyperintense T2  
206 white matter signal (periventricular leukomalacia) on MRI, spastic-dystonic diplegia,  
207 expressive language disorder, and aortic arch abnormalities (**Fig. 1c**, **Supplementary**  
208 **Table 4**, and **Supplementary Videos F064** and **F244**). *RHOB* is known to control  
209 dendritic spine outgrowth<sup>34</sup> but has not previously been associated with a human  
210 disease. Biochemical analyses indicated that this variant shows accentuated responses  
211 to both GTPase activating proteins (GAPs) and GDP exchange factors (GEFs) (**Fig.**  
212 **1d,e**), ultimately leading to enhanced binding in the active state to the Rho effector  
213 rhotekin (**Fig. 1f**).

214 We also identified two unrelated cases with an identical DNM (p.Asp334Asn; **Fig.**  
215 **2a** and **Supplementary Table 4**) in *FBXO31*, which encodes the F-box only protein 31.  
216 An *FBXO31*/SKP1/Cullin1 complex ubiquitinates targets such as cyclin D to control  
217 protein abundance by tagging for proteasomal degradation<sup>35</sup>. Asp334 is a conserved  
218 residue within the binding pocket on *FBXO31* (**Fig. 2b**), where it is thought to mediate  
219 hydrogen bonding to cyclin D1<sup>36</sup>. *FBXO31* is known to control axonal outgrowth and is  
220 essential for dendrite growth and neuronal migration in the developing brain<sup>37</sup>. *FBXO31*  
221 p.Asp334Asn affects the cyclin D interaction site<sup>36</sup> (**Fig. 2b**), leading to an apparent gain  
222 of function of cyclin D degradation (**Fig. 2c**). A homozygous truncating mutation in  
223 *FBXO31* has previously been reported in association with intellectual disability (OMIM#  
224 615979)<sup>38</sup>. Both patients in our cohort exhibited spastic diplegic CP (**Supplementary**  
225 **Table 4** and **Supplementary Videos F218** and **F699**), intellectual disability, expressive  
226 language disorder, and ADHD. F218 had gut malrotation and constipation, cleft palate,  
227 strabismus, and normal brain morphology on MRI, while F699 had strabismus, severe

228 constipation, and ventricular dilation with thin corpus callosum on MRI. Therefore, this  
229 DNM in *FBXO31* leads to a phenotype distinct from the previously described autosomal  
230 recessive truncating mutation-associated nonsyndromic intellectual disability  
231 phenotype<sup>38</sup>.

232  
233 **DNMs in previously implicated genes *TUBA1A*, *CTNNB1*, *ATL1*, and *SPAST*.**  
234 *TUBA1A*, encoding the microtubule-related protein  $\alpha$ -tubulin, harbors three damaging  
235 DNMs (p.Arg123Cys, p.Leu152Gln, p.Tyr408Asp; **Supplementary Table 4**) in three  
236 unrelated probands, two of whom have been previously reported<sup>22</sup>. Both p.Arg123Cys  
237 and p.Leu152Gln map to the tubulin nucleotide binding domain-like, and p.Tyr408Asp  
238 maps to the C-terminal stabilization domain<sup>39</sup> (**Extended Data Fig. 3**). *TUBA1A*  
239 heterozygous mutations have been described as associated with a spectrum of cortical  
240 malformations<sup>40</sup> (OMIM# 611603), and our patients exhibit MRI findings within this  
241 spectrum (**Extended Data Fig. 3**). Clinically, our cases demonstrate spasticity in their  
242 lower limbs, and 2/3 exhibit concurrent intellectual disability.

243 *CTNNB1*, encoding  $\beta$ -catenin, harbors three LoF DNMs (p.Glu54\*,  
244 p.Phe99PhefsTer5, p.Arg449GlnfsTer24; **Supplementary Table 4**) in three unrelated  
245 probands, one of whom was previously reported<sup>21</sup>. p.Glu54\* and p.Phe99fs are located  
246 in the N-terminal domain and predicted to lead to nonsense-mediated decay, while  
247 p.Arg449fs is located in the central armadillo repeat domain, which is essential for the  
248 phosphorylation of  $\beta$ -catenin by protein kinase CK2<sup>41</sup> (**Extended Data Fig. 4**).  
249 Autosomal dominant germline inactivating mutations in *CTNNB1* have been implicated  
250 in exudative vitreoretinopathy 7<sup>42</sup> (OMIM# 617572) and neurodevelopmental disorder  
251 with spastic diplegia and visual defects<sup>43-45</sup> (OMIM# 615075). All of our patients  
252 exhibited spasticity, intellectual disability, behavior problems and language disorders.  
253 We also found dystonia and microcephaly in 2/3 patients. While one patient had  
254 possible bilateral frontal pachygyria, brain findings were notably absent from the other  
255 patients (**Extended Data Fig. 4**). We found strabismus in 2/3 patients, but no other  
256 visual defects.

257 *ATL1* encodes atlastin-1, which is critical for formation of the tubular endoplasmic  
258 reticulum network and axon elongation in neurons<sup>46-48</sup>. *ATL1* harbors two damaging  
259 DNMs in our cohort (p.Ala350Val, p.Lys406Gln; **Supplementary Table 4**) located in the  
260 GBP domain (**Extended Data Fig. 5**). Autosomal dominant germline mutations have  
261 been associated with neuropathy type 1D<sup>49</sup> (OMIM# 613708) and spastic paraplegia  
262 type 3A<sup>50</sup> (OMIM# 182600). Our patients exhibited spasticity and dystonia with brain  
263 findings of T2 hyperintensities and bihemispheric periventricular leukomalacia  
264 (**Extended Data Fig. 5**). There was no evidence of phenotypic progression at the time  
265 of last follow-up (patient ages 10 years and 29 months).

266 *SPAST*, encoding spastin, harbored two damaging DNMs (p.Asp441Gly,  
267 p.Ala495Pro; **Supplementary Table 4**). Both mutations occur at conserved positions in  
268 the AAA domain, which is essential for the regulation of ATPase activity (**Extended**  
269 **Data Fig. 6**). Autosomal dominant germline mutations in *SPAST* have been linked to  
270 spastic paraplegia 4<sup>51</sup> (OMIM# 182601). p.Asp441Gly has been reported in association  
271 with hereditary spastic paraplegia (HSP)<sup>52,53</sup>. Our patients exhibited spasticity with one  
272 also exhibiting dystonia, with scattered subcortical T2 hyperintensities present in one  
273 patient and no brain findings in the other (**Extended Data Fig. 6**). There was no



274 evidence of phenotypic progression (patient ages 21 years and 40 months,  
275 respectively).

276  
277 **DNMs in *DHX32* and *ALK*.** *DHX32*, encoding putative pre-mRNA-splicing factor ATP-  
278 dependent RNA helicase *DHX32*, harbored two damaging DNMs (p.Tyr228Cys,  
279 p.Ile266Met; **Supplementary Table 4**). p.Tyr228Cys falls within the helicase ATP  
280 binding domain, which is required for ATP binding, hydrolysis, and nucleic acid  
281 substrate binding<sup>54</sup> (**Extended Data Fig. 7**). Mutations in *DHX32* have not previously  
282 been associated with human diseases. Both of our patients exhibited intellectual  
283 disability, and one demonstrated spastic diplegia, with the other characterized as a  
284 generalized dystonia. Brain findings included periventricular leukomalacia and mildly  
285 diminished cerebral volume (**Extended Data Fig. 7**).

286 *ALK*, encoding ALK receptor tyrosine kinase, harbored one damaging DNM  
287 (p.Ser1081Arg) and one stop-gain DNM (p.Trp1320\*) (**Supplementary Table 4**).  
288 p.Trp1320\* is located in the tyrosine kinase domain<sup>55</sup> and p.Ser1081Arg is located just  
289 upstream in the juxtamembrane domain (**Extended Data Fig. 8**). Germline and somatic  
290 activating mutations in *ALK* have been previously associated with neuroblastoma<sup>56,57</sup>  
291 (OMIM# 613014). One patient exhibited spastic diplegia with mild tremor, scattered  
292 subcortical hyperintensities (**Extended Data Fig. 8**), and an atrial septal defect. The  
293 other patient had spastic-dystonic diplegia, white matter abnormalities, and epilepsy.  
294 There was no evidence of neuroblastoma in either patient.

295  
296 **Enriched recessive genotypes in genes associated with hereditary spastic**  
297 **paraplegia.** We performed a one-tailed binomial test coupled with a polynomial model<sup>24</sup>  
298 to evaluate the burden of recessive genotypes (RGs) for each gene in our CP cohort  
299 (**Supplementary Data Set 3**). We did not observe enrichment of damaging RGs in the  
300 cohort meeting genome-wide significance (**Supplementary Table 6**). However, we  
301 noted biallelic damaging variants in several genes previously associated with HSP. HSP  
302 is clinically distinguished from CP by its progressive, neurodegenerative nature and  
303 later (often adult) onset in many cases.

304 We carefully re-assessed clinical phenotypes of these cases and found no  
305 evidence of progression from the time of ascertainment. Interestingly, early-onset with  
306 protracted clinical stability has previously been identified as an endophenotype in a  
307 subset of patients with mutations in HSP-associated genes<sup>58</sup>. For example, patients with  
308 *SPAST* missense mutations (as our cases did) may have onset in toddlerhood with  
309 extended clinical stability<sup>59</sup> consistent with a CP phenotype. In contrast, truncating  
310 *SPAST* mutations are often translated and accumulate over time, putatively leading to  
311 later-onset and a neurodegenerative course<sup>60</sup>. In addition, important roles for *SPAST*<sup>61</sup>  
312 and *ATL1*<sup>62</sup> in developmental neuritogenesis have been shown, indicating their  
313 importance in neuronal development.

314 We observed six damaging RGs (in *AMPD2*, *AP4M1*, *AP5Z1*, *FARS2*, *NT5C2*,  
315 and *SPG11*; **Supplementary Table 7**) among genes previously associated with  
316 recessive HSP (**Supplementary Data Set 4**) (enrichment = 7.74; one-tailed binomial  $P$   
317 =  $1.5 \times 10^{-4}$ ; **Table 3**). By ascertainment differential, ~2.1% of the CP cases in our  
318 cohort could thus be accounted for by an excess of RGs. The enrichment of RGs in  
319 known HSP-associated genes was predominantly driven by idiopathic cases (idiopathic

320 enrichment = 9.22; one-tailed binomial  $P = 2.4 \times 10^{-4}$  vs. environment enrichment =  
321 4.48; one-tailed binomial  $P = 0.20$ ; **Table 3**).

322  
323 **No gene was enriched for rare X-linked hemizygous variants.** Male sex is a risk  
324 factor for developing CP<sup>63</sup>. Therefore, we compared rare hemizygous variants (MAF  $\leq$   
325  $5.0 \times 10^{-5}$ ) in 154 male CP probands to male controls in gnomAD. No gene surpassed  
326 Bonferroni correction cutoff (**Supplementary Table 8**), suggesting that the current study  
327 is statistically underpowered to assess hemizygous burden.

328  
329 **Clinical and genetic overlap of CP with other neurodevelopmental disorders.**  
330 Clinically, NDDs frequently co-occur. In the case of CP, ~45% of individuals with CP  
331 have concurrent ID<sup>64</sup>, ~40% also have epilepsy, and ~7% have ASD in addition to CP<sup>1</sup>.  
332 Accordingly, we sought to determine the degree of overlap between genes harboring  
333 rare damaging variants with *de novo*, X-linked recessive, or autosomal recessive  
334 segregation (putative CP risk genes;  $n = 439$ , **Supplementary Data Sets 6-15**) from our  
335 CP cohort with known NDD risk genes. The analysis was performed using the Disease  
336 Gene Network, which identifies associations between genes and diseases curated from  
337 the literature and databases including ClinVar, ClinGen, and UniProt<sup>65</sup>. We found  
338 substantial genetic overlap between our CP candidate gene list and the major NDDs  
339 (CP vs. ID, enrichment = 2.0,  $P = 2.56 \times 10^{-16}$ ; CP vs. epilepsy, enrichment = 1.7,  $P =$   
340  $1.6 \times 10^{-4}$ ; CP vs. ASD, enrichment = 2.0,  $P = 1.2 \times 10^{-5}$ , hypergeometric two-tailed test)  
341 (**Fig. 3a**). In contrast, when we examined overlap with a neurodegenerative disorder,  
342 Alzheimer's disease, there was no enrichment (**Fig. 3b**). 28.9% of CP risk genes  
343 overlapped with genes linked to ID, 11.1% for epilepsy, and 6.3% for ASD. Our data  
344 suggest that CP has significant genetic overlap with other genetic neurodevelopmental  
345 disorders, indicating potential genetic pleiotropy and common etiologies of co-occurring  
346 NDDs.

347  
348 **Extracellular matrix, cell-matrix focal adhesions, the cytoskeletal network, and**  
349 **Rho GTPase genes are highly associated with CP.** We identified a large number of  
350 individual genes harboring predicted damaging variants and employed a suite of tools  
351 for unbiased discovery of conserved pathways and biological functions relevant to CP.  
352 STRING-based clustering<sup>66</sup> of the 439 putative CP risk genes (**Supplementary Data**  
353 **Sets 6-15**) showed greater connectivity than predicted by chance (enrichment = 1.2,  $P =$   
354  $1.51 \times 10^{-4}$ ) indicating a functional network encompassing damaging variants. We then  
355 performed gene over-representation analysis (ORA)<sup>67,68</sup> of these genes using DAVID<sup>69</sup>,  
356 MSigDB<sup>70</sup> and PANTHER<sup>71</sup> for functional annotation and pathway characterization. This  
357 approach indicated statistical over-representation of candidate genes stratified by Gene  
358 Ontology (GO), pathways (KEGG/Reactome), and curated functional and expression  
359 data to identify meaningful relationships. Consistent with the STRING findings, this  
360 approach identified multiple gene sets representing enriched pathways (false discovery  
361 rate (FDR)  $< 0.05$ ) and conserved functions (**Supplementary Data Sets 6-15**).

362 We noted functionally related findings supported by multiple tools, including non-  
363 integrin membrane-extracellular matrix (ECM) interactions and laminin interaction  
364 pathways identified by all three algorithms. We then inferred hierarchical associations  
365 between ontological terms using dcGO<sup>72</sup> (**Table 4**). Taken together, these findings

366 indicate an over-representation of genes involved in extracellular matrix biology, cell-  
367 matrix interactions (focal adhesions), cytoskeletal dynamics and Rho GTPase function.

368

369 **Genes from Rho GTPase, cytoskeleton, and cell projection pathways govern**  
370 **neuromotor development in Drosophila.** Subsequently, we independently assessed  
371 the role for over-represented pathway members in normal locomotor development by  
372 conducting a reverse genetic screen in Drosophila. A similar approach has been applied  
373 previously in studies of ASD and HSP using Drosophila and zebrafish, respectively<sup>73,74</sup>.  
374 We focused on genes with damaging variants from our CP patient cohort with GTPase,  
375 cytoskeleton, and cell projection GO terms. We hypothesized that our screen could  
376 newly indicate a key role for these genes in neuromotor development.

377 We selected genes with conserved Drosophila orthologs (DIOPT  $\geq 5$ ) that had  
378 available molecularly characterized alleles (complete results and genotypes in  
379 **Supplementary Table 9**). We utilized hypomorphic/LoF alleles in a biallelic state to  
380 help map phenotypes to the gene of interest in Drosophila assays. We excluded genes  
381 that would cause confounding phenotypes such as lethality or had a previously  
382 described locomotor phenotype, except for *ATL1*, which was included as a positive  
383 control. Genes with known roles in brain development or NDDs were prioritized. Two  
384 genes with variants that did not meet the filtering criteria for deleteriousness were  
385 included as negative controls. Altogether, we screened 22 genes for locomotor ability  
386 using turning assays in larvae<sup>75</sup> and negative geotaxis/positive phototaxis assays in  
387 adults<sup>76,77</sup>.

388 We found locomotor phenotypes in mutants of gene orthologs encoding  
389 regulators of GTPase signal transduction (*AGAP1*, *DOCK11*, *RABEP1*, *SYNGAP1*,  
390 *TBC1D17*), the cytoskeleton (*MKL1*, *MPP1*), and cell projection (*PTK2B*, *SEMA4A*,  
391 *TENM1*) pathways (**Fig. 4**). When assays were conducted in both larvae and adults, we  
392 often found locomotor phenotypes at both timepoints, suggesting that defects arose in  
393 the developmental period and persisted throughout the lifespan (**Supplementary Table**  
394 **9**). Of potential interest, we found evidence for sexual dimorphism as male flies with  
395 mutations in orthologs of *AKT3*, *RABEP1*, or *PRICKLE1/2* exhibited locomotor deficits  
396 while females did not.

397 In total, we found 71% (10/14) genes from our enriched pathways exhibited a  
398 locomotor phenotype in Drosophila (**Fig. 4** and **Extended Data Fig. 9**). In comparison,  
399 genome-wide, only 3.1% of annotated Drosophila genes are known to lead to a  
400 locomotor phenotype<sup>78</sup> (enrichment = 23.4,  $P = 2.2 \times 10^{-16}$ ; **Fig. 4**). Overall, our  
401 Drosophila studies supported a role for candidate CP genes in the cytoskeletal, Rho  
402 GTPase, and cell projection pathways in motor development.

403

404

## 405 **DISCUSSION**

406

407 In the past, damaging genomic variants have not been considered to be a major  
408 contributor to CP, but our findings and those of others challenge this dogma. Prior  
409 studies suggested that both CNVs and single nucleotide variants contribute to CP<sup>10,16-22</sup>.  
410 Here we expand upon those earlier findings and provide robust statistical evidence at a  
411 cohort level that rare, damaging single nucleotide variants represent an independent

412 risk factor for CP. The cohort-wide enrichment of DNMs we detected is consistent with  
413 the observation that most cases of CP occur sporadically<sup>79</sup>. Using the distribution of  
414 LoF-intolerant genes with multiple damaging DNMs in this cohort, we estimated the  
415 number of genes that contribute to CP through a *de novo* mechanism to be 75 (95%  
416 confidence interval = (26.5, 123.5)) (**Extended Data Fig. 10a** and **Supplementary**  
417 **Note**). Saturation analysis estimates that WES of 2,500 and 7,500 CP trios will yield  
418 65.3% and 91.8% saturation, respectively, for CP risk genes with DNMs, suggesting a  
419 high yield for CP gene discovery as additional samples are sequenced (**Extended Data**  
420 **Fig. 10b**). Accordingly, the International Cerebral Palsy Genomics Consortium (ICPGC;  
421 [www.icpgc.org](http://www.icpgc.org)) was recently founded to address the need for international data sharing  
422 and collaboration to advance the pace of discovery<sup>80</sup>. Conservatively, we estimate that  
423 14% of the cases in our cohort can be accounted for by damaging genomic variants  
424 (based on ascertainment differentials of 11.9% for DNMs and ~2% for RGs). In  
425 comparison, recent estimates indicate that acute intrapartum hypoxia-ischemia is seen  
426 in ~6% of CP cases<sup>81</sup>, indicating that genomic mutations represent an important,  
427 independent contributor to CP etiology that historically has been overlooked.

428 We found evidence for both known disease-associated genes and genes not  
429 previously associated with human phenotypes in our cohort. The identification of  
430 independently arising yet identical DNMs in *RHOB* and *FBXO31* indicates that  
431 monogenic contributions to CP exist but may be under-recognized. Our parallel  
432 identification of genetic correlation of CP with other NDDs implicates shared  
433 susceptibility as suggested previously<sup>82</sup>. In some cases, this may reflect ascertainment  
434 bias, as motor phenotypes may have been under-reported in prior studies of other  
435 NDDs. In other cases, typified by *FBXO31*, our findings likely represent phenotypic  
436 expansions. Finally, in some contexts, NDD manifestations may prove pleiotropic, with a  
437 genetic disruption of early neurodevelopment manifesting variably as is increasingly  
438 being recognized<sup>83</sup>. Analogous to other NDDs, individual CP cases may prove to be  
439 environmental in origin, genetic, or some combination thereof. However, somewhat  
440 uniquely among the NDDs, environmental contributions to CP are relatively well  
441 characterized, and CP may represent a model disorder within which to study gene-  
442 environment interactions in a developmental context.

443 Altered motor circuit connectivity is thought to be part of CP pathophysiology<sup>84</sup>.  
444 By integrating orthogonal lines of evidence, including recurrent gene analyses, *in vitro*  
445 and *in vivo* functional assays, cohort-wide network biology approaches, and *Drosophila*  
446 locomotor studies, we found converging evidence supporting a role for extracellular  
447 matrix components, cell-matrix focal adhesions, cytoskeletal organization and Rho  
448 GTPases in CP etiology. These processes are known to drive the conserved process of  
449 cell projection extensions during nervous system development<sup>85</sup>. Based on known  
450 disease and developmental biology, we therefore predict that disruption of genes  
451 involved in neurodevelopmental patterning may alter early neuritogenesis and neuronal  
452 functional network connectivity in CP. Further studies will be needed to determine more  
453 specifically how CP patient-derived variants affect neuronal circuit development.

454 Our findings have important clinical implications. Specific genetic findings may  
455 provide closure for families and guide preventative healthcare as well as family  
456 planning, such as counseling for recurrence risk (often quoted as ~1% for CP but  
457 potentially much higher for inherited mutations). In some cases, identification of specific

458 variants in individuals in our cohort led to recommendations for changes in  
459 management, including personalized treatments that would not otherwise have been  
460 initiated (i.e. ethosuximide for *GNB*<sup>86</sup> (F068), levodopa for *CTNNB1*<sup>87</sup> (F066, GRA8913,  
461 F428), and 5-aminoimidazole-4-carboxamide riboside (AICAr) for *AMPD*<sup>88</sup> (F623)  
462 **(Supplementary Note)**.

463 In the near future, studies will be able to overcome our limitations of small  
464 sample size and further utilize available clinical data to expand upon genotype-  
465 phenotype correlations. Additionally, as more information about CP genetic etiology  
466 becomes available, it will become possible to assign likely genetic causation to more  
467 individual cases. Future studies of well-characterized unselected CP cohorts will be  
468 instrumental in determining the true contributions of genetic and environmental factors  
469 side-by-side in order to clarify the epidemiology of CP.

470 Overall, our data indicate that genomic variants should be considered alongside  
471 environmental insults when assessing the etiology of an individual's CP. Such  
472 considerations will have important clinical, research, and medico-legal implications. In  
473 the near future, genomic data may help stratify patients and identify likely responders to  
474 currently available medical and/or surgical therapies. Finally, over time, mechanistic  
475 insights derived from the identification of core pathways via genomic studies of CP may  
476 help guide therapeutic development efforts in a field that has not seen a novel therapy  
477 introduced for decades.

478

479 **ACKNOWLEDGEMENTS**

480

481 We gratefully acknowledge the support of the patients and families who have  
482 graciously and patiently supported this work from its inception. Without their partnership,  
483 these studies would not have been possible. We acknowledge the support of the  
484 clinicians who generously provided their expertise in support of this study, including  
485 Mary-Claire Waugh, Matthias Axt, and Vicki Roberts of the Children’s Hospital  
486 Westmead; Kevin Lowe of Sydney Children’s Hospital; Ray Russo, James Rice, and  
487 Andrew Tidemann of the Women’s and Children’s Hospital, Adelaide; Theresa Carroll  
488 and Lisa Copeland of the Lady Cilento Children’s Hospital, Brisbane; and Jane  
489 Valentine of Perth Children’s Hospital. We appreciate the collaboration of Susan  
490 Knoblach and Eric Hoffman (Children’s National Medical Center).

491 This work was supported in part by the Cerebral Palsy Alliance Research  
492 Foundation (M.C.K.), the Yale-NIH Center for Mendelian Genomics (U54 HG006504-  
493 01), Doris Duke Charitable Foundation CSDA 2014112 (M.C.K.), the Scott Family  
494 Foundation (M.C.K.), Cure CP (M.C.K.), 5R24HD050846-08 (E.P.H.), NHMRC grant  
495 1099163 (A.H.M., C.L.v.E., J.G., and M.A.C.), Cerebral Palsy Alliance Research  
496 Foundation Career Development Award (M.A.C.), the Tenix Foundation (A.H.M., J.G.,  
497 C.L.v.E., and M.A.C.), the National Natural Science Foundation of China (U1604165,  
498 X.W.), Henan Key Research Program of China (171100310200, C. Zhu), VINNOVA  
499 (2015-04780, C. Zhu), the James Hudson Brown-Alexander Brown Coxe Postdoctoral  
500 Fellowship at the Yale University School of Medicine (S.C.J.), an American Heart  
501 Association Postdoctoral Fellowship (18POST34060008 to S.C.J.), the NIH K99/R00  
502 Pathway to Independence Award (R00HL143036-02 to S.C.J.) and NIH grants  
503 R01NS091299 (D.C.Z.) and NIH R01NS106298 (M.C.K.).

504

505

506 **AUTHOR CONTRIBUTIONS**

507

508 K.B., S.P.-L., Q.X., C. Zhu, R.P.L., A.H.M., J.G., and M.C.K. contributed to study design,  
509 data interpretation, and oversight. B.Y.N., J.G.B., K.H., C. Zhou, D.Z., B.Z, B.K., S.W.,  
510 J.B., S.P., J.B.V., J.B.-H., A.P., M.C.F., L.X., Y.X., M.C., K.R., F.M., Y.W., J.L.W., L.R.,  
511 J.S.C., A.F., A.E.L., J.P.P., T.F., S.J.M., K.E.C., S.M.R., D.S.R., Q.S., C.G., Y.A.W.,  
512 N.B., I.N., S.C.M., X.W., D.J.A., J.H., and M.C.K. provided cohort ascertainment,  
513 recruitment, and phenotypic characterization. K.B., C.C., A.E., J.L., C.L.v.E., H.M.,  
514 S.M.M., I.R.T., F.L.-G., Y.A.W., B.S.G., J.Z., D.L.W., M.S.B.F., C. Zhou, and M.A.C.  
515 performed exome sequencing production and validation. S.B., S.C.J., M.A.C., M.C.S.,  
516 X.Z., J.R.K., and A.H.S. performed WES analysis. A.E., H.M., J.L., B.S.G., and S.P.-L.  
517 performed RHOB validation. S.M.N., S.P.-L., S.P., J.B.V., D.D., and S.A.L. performed  
518 FBXO31 validation. S.A.L., S.V., and D.C.Z. performed Drosophila locomotor  
519 experiments. S.C.J., S.A.L., S.B., S.S., B.L., Q.L., M.C.S., and X.Z. conducted statistical  
520 analysis. S.H. performed biophysical simulation for RHOB and FBXO31. S.C.J., S.A.L.,  
521 J.G., Q.L., S.P.-L., R.P.L., A.H.M., S.M., B.Y.N., M.C.S., X.Z., C.L.v.E., X.W., Q.X., C.  
522 Zhu, and M.C.K. wrote and reviewed manuscript. K.B., R.P.L., Q.X., C. Zhu, A.H.M.,  
523 J.G., S.P.-L., and M.C.K. acquired funding and supervised the project and were  
524 considered co-senior authors. All authors have read and approved the final manuscript.

525

526 **COMPETING INTERESTS**

527

528 None

529

530

531 **REFERENCES**

532

- 533 1. Christensen, D. *et al.* Prevalence of cerebral palsy, co-occurring autism spectrum  
534 disorders, and motor functioning - Autism and Developmental Disabilities  
535 Monitoring Network, USA, 2008. *Dev. Med. Child Neurol.* **56**, 59-65 (2014).
- 536 2. Oskoui, M., Coutinho, F., Dykeman, J., Jette, N. & Pringsheim, T. An update on  
537 the prevalence of cerebral palsy: a systematic review and meta-analysis. *Dev.*  
538 *Med. Child Neurol.* **55**, 509-519 (2013).
- 539 3. Surveillance of Cerebral Palsy in, E. Surveillance of cerebral palsy in Europe: a  
540 collaboration of cerebral palsy surveys and registers. Surveillance of Cerebral  
541 Palsy in Europe (SCPE). *Dev. Med. Child Neurol.* **42**, 816-824 (2000).
- 542 4. Longo, L.D. & Ashwal, S. William Osler, Sigmund Freud and the evolution of  
543 ideas concerning cerebral palsy. *J. Hist. Neurosci.* **2**, 255-282 (1993).
- 544 5. Panteliadis, C., Panteliadis, P. & Vassilyadi, F. Hallmarks in the history of  
545 cerebral palsy: from antiquity to mid-20th century. *Brain Dev.* **35**, 285-292 (2013).
- 546 6. Tan, S. Fault and blame, insults to the perinatal brain may be remote from time of  
547 birth. *Clin. Perinatol.* **41**, 105-117 (2014).
- 548 7. Donn, S.M., Chiswick, M.L. & Fanaroff, J.M. Medico-legal implications of hypoxic-  
549 ischemic birth injury. *Semin. Fetal Neonatal Med.* **19**, 317-321 (2014).
- 550 8. Korzeniewski, S.J., Slaughter, J., Lenski, M., Haak, P. & Paneth, N. The complex  
551 aetiology of cerebral palsy. *Nat. Rev. Neurol.* **14**, 528-543 (2018).
- 552 9. Numata, Y. *et al.* Brain magnetic resonance imaging and motor and intellectual  
553 functioning in 86 patients born at term with spastic diplegia. *Dev. Med. Child*  
554 *Neurol.* **55**, 167-172 (2013).
- 555 10. Segel, R. *et al.* Copy number variations in cryptogenic cerebral palsy. *Neurology*  
556 **84**, 1660-1668 (2015).
- 557 11. McIntyre, S. *et al.* Congenital anomalies in cerebral palsy: where to from here?  
558 *Dev. Med. Child Neurol.* **58 Suppl 2**, 71-75 (2016).
- 559 12. Petterson, B., Stanley, F. & Henderson, D. Cerebral palsy in multiple births in  
560 Western Australia: genetic aspects. *Am. J. Med. Genet.* **37**, 346-351 (1990).
- 561 13. Costeff, H. Estimated frequency of genetic and nongenetic causes of congenital  
562 idiopathic cerebral palsy in west Sweden. *Ann. Hum. Genet.* **68**, 515-520 (2004).
- 563 14. Hallmayer, J. *et al.* Genetic heritability and shared environmental factors among  
564 twin pairs with autism. *Arch. Gen. Psychiatry* **68**, 1095-1102 (2011).
- 565 15. Sandin, S. *et al.* The heritability of autism spectrum disorder. *JAMA* **318**, 1182-  
566 1184 (2017).
- 567 16. McMichael, G. *et al.* Rare copy number variation in cerebral palsy. *Eur. J. Hum.*  
568 *Genet.* **22**, 40-45 (2014).
- 569 17. Oskoui, M. *et al.* Clinically relevant copy number variations detected in cerebral  
570 palsy. *Nat. Commun.* **6**, 7949 (2015).
- 571 18. Zarrei, M. *et al.* De novo and rare inherited copy-number variations in the  
572 hemiplegic form of cerebral palsy. *Genet. Med.* **20**, 172-180 (2018).

- 573 19. Corbett, M.A. *et al.* Pathogenic copy number variants that affect gene expression  
574 contribute to genomic burden in cerebral palsy. *NPJ Genom. Med.* **3**, 33 (2018).
- 575 20. Takezawa, Y. *et al.* Genomic analysis identifies masqueraders of full-term  
576 cerebral palsy. *Ann. Clin. Transl. Neurol.* **5**, 538-551 (2018).
- 577 21. Parolin Schneckenberg, R. *et al.* De novo point mutations in patients diagnosed  
578 with ataxic cerebral palsy. *Brain* **138**, 1817-1832 (2015).
- 579 22. McMichael, G. *et al.* Whole-exome sequencing points to considerable genetic  
580 heterogeneity of cerebral palsy. *Mol. Psychiatry* **20**, 176-182 (2015).
- 581 23. Rosenbaum, P. *et al.* A report: the definition and classification of cerebral palsy  
582 April 2006. *Dev. Med. Child Neurol. Suppl.* **109**, 8-14 (2007).
- 583 24. Jin, S.C. *et al.* Contribution of rare inherited and de novo variants in 2,871  
584 congenital heart disease probands. *Nat. Genet.* **49**, 1593-1601 (2017).
- 585 25. Krumm, N. *et al.* Excess of rare, inherited truncating mutations in autism. *Nat.*  
586 *Genet.* **47**, 582-588 (2015).
- 587 26. McKenna, A. *et al.* The Genome Analysis Toolkit: a MapReduce framework for  
588 analyzing next-generation DNA sequencing data. *Genome Res.* **20**, 1297-1303  
589 (2010).
- 590 27. Van der Auwera, G.A. *et al.* From FastQ data to high confidence variant calls: the  
591 Genome Analysis Toolkit best practices pipeline. *Curr. Protoc. Bioinformatics* **43**,  
592 11 10 1-33 (2013).
- 593 28. Dong, C. *et al.* Comparison and integration of deleteriousness prediction  
594 methods for nonsynonymous SNVs in whole exome sequencing studies. *Hum.*  
595 *Mol. Genet.* **24**, 2125-2137 (2015).
- 596 29. Kircher, M. *et al.* A general framework for estimating the relative pathogenicity of  
597 human genetic variants. *Nat. Genet.* **46**, 310-315 (2014).
- 598 30. Wei, Q. *et al.* A Bayesian framework for de novo mutation calling in parents-  
599 offspring trios. *Bioinformatics* **31**, 1375-1381 (2015).
- 600 31. Karczewski, K.J. *et al.* The mutational constraint spectrum quantified from  
601 variation in 141,456 humans. *Nature* **581**, 434-443 (2020).
- 602 32. Rainier, S., Sher, C., Reish, O., Thomas, D. & Fink, J.K. De novo occurrence of  
603 novel SPG3A/atlastin mutation presenting as cerebral palsy. *Arch. Neurol.* **63**,  
604 445-447 (2006).
- 605 33. Blom, N., Gammeltoft, S. & Brunak, S. Sequence and structure-based prediction  
606 of eukaryotic protein phosphorylation sites. *J. Mol. Biol.* **294**, 1351-1362 (1999).
- 607 34. McNair, K. *et al.* A role for RhoB in synaptic plasticity and the regulation of  
608 neuronal morphology. *J. Neurosci.* **30**, 3508-3517 (2010).
- 609 35. Deshaies, R.J. & Joazeiro, C.A. RING domain E3 ubiquitin ligases. *Annu. Rev.*  
610 *Biochem.* **78**, 399-434 (2009).
- 611 36. Li, Y. *et al.* Structural basis of the phosphorylation-independent recognition of  
612 cyclin D1 by the SCF(FBXO31) ubiquitin ligase. *Proc. Natl. Acad. Sci. USA* **115**,  
613 319-324 (2018).
- 614 37. Vadhvani, M., Schwedhelm-Domeyer, N., Mukherjee, C. & Stegmuller, J. The  
615 centrosomal E3 ubiquitin ligase FBXO31-SCF regulates neuronal morphogenesis  
616 and migration. *PLoS One* **8**, e57530 (2013).



- 617 38. Mir, A. *et al.* Truncation of the E3 ubiquitin ligase component FBXO31 causes  
618 non-syndromic autosomal recessive intellectual disability in a Pakistani family.  
619 *Hum. Genet.* **133**, 975-984 (2014).
- 620 39. Lefevre, J. *et al.* The C terminus of tubulin, a versatile partner for cationic  
621 molecules: binding of Tau, polyamines, and calcium. *J. Biol. Chem.* **286**, 3065-  
622 3078 (2011).
- 623 40. Hebebrand, M. *et al.* The mutational and phenotypic spectrum of TUBA1A-  
624 associated tubulinopathy. *Orphanet J. Rare Dis.* **14**, 38 (2019).
- 625 41. Song, D.H. *et al.* CK2 phosphorylation of the armadillo repeat region of beta-  
626 catenin potentiates Wnt signaling. *J. Biol. Chem.* **278**, 24018-24025 (2003).
- 627 42. Panagiotou, E.S. *et al.* Defects in the cell signaling mediator beta-catenin cause  
628 the retinal vascular condition FEVR. *Am. J. Hum. Genet.* **100**, 960-968 (2017).
- 629 43. de Ligt, J. *et al.* Diagnostic exome sequencing in persons with severe intellectual  
630 disability. *N. Engl. J. Med.* **367**, 1921-1929 (2012).
- 631 44. Tucci, V. *et al.* Dominant beta-catenin mutations cause intellectual disability with  
632 recognizable syndromic features. *J. Clin. Invest.* **124**, 1468-1482 (2014).
- 633 45. Kharbanda, M. *et al.* Clinical features associated with CTNNB1 de novo loss of  
634 function mutations in ten individuals. *Eur. J. Med. Genet.* **60**, 130-135 (2017).
- 635 46. Chen, J., Knowles, H.J., Hebert, J.L. & Hackett, B.P. Mutation of the mouse  
636 hepatocyte nuclear factor/forkhead homologue 4 gene results in an absence of  
637 cilia and random left-right asymmetry. *J. Clin. Invest.* **102**, 1077-1082 (1998).
- 638 47. Orso, G. *et al.* Homotypic fusion of ER membranes requires the dynamin-like  
639 GTPase atlastin. *Nature* **460**, 978-983 (2009).
- 640 48. Zhu, P.P., Denton, K.R., Pierson, T.M., Li, X.J. & Blackstone, C. Pharmacologic  
641 rescue of axon growth defects in a human iPSC model of hereditary spastic  
642 paraplegia SPG3A. *Hum. Mol. Genet.* **23**, 5638-5648 (2014).
- 643 49. Guelly, C. *et al.* Targeted high-throughput sequencing identifies mutations in  
644 atlastin-1 as a cause of hereditary sensory neuropathy type I. *Am. J. Hum.*  
645 *Genet.* **88**, 99-105 (2011).
- 646 50. Zhao, X. *et al.* Mutations in a newly identified GTPase gene cause autosomal  
647 dominant hereditary spastic paraplegia. *Nat. Genet.* **29**, 326-331 (2001).
- 648 51. Hazan, J. *et al.* Spastin, a new AAA protein, is altered in the most frequent form  
649 of autosomal dominant spastic paraplegia. *Nat. Genet.* **23**, 296-303 (1999).
- 650 52. Burger, J. *et al.* Hereditary spastic paraplegia caused by mutations in the SPG4  
651 gene. *Eur. J. Hum. Genet.* **8**, 771-776 (2000).
- 652 53. Hazan, J. *et al.* A fine integrated map of the SPG4 locus excludes an expanded  
653 CAG repeat in chromosome 2p-linked autosomal dominant spastic paraplegia.  
654 *Genomics* **60**, 309-319 (1999).
- 655 54. de la Cruz, J., Kressler, D. & Linder, P. Unwinding RNA in *Saccharomyces*  
656 *cerevisiae*: DEAD-box proteins and related families. *Trends Biochem. Sci.* **24**,  
657 192-198 (1999).
- 658 55. Della Corte, C.M. *et al.* Role and targeting of anaplastic lymphoma kinase in  
659 cancer. *Mol. Cancer* **17**, 30 (2018).
- 660 56. Chen, Y. *et al.* Oncogenic mutations of ALK kinase in neuroblastoma. *Nature*  
661 **455**, 971-974 (2008).

- 662 57. Janoueix-Lerosey, I. *et al.* Somatic and germline activating mutations of the ALK  
663 kinase receptor in neuroblastoma. *Nature* **455**, 967-970 (2008).
- 664 58. Schule, R. *et al.* Hereditary spastic paraplegia: clinicogenetic lessons from 608  
665 patients. *Ann. Neurol.* **79**, 646-658 (2016).
- 666 59. Parodi, L. *et al.* Spastic paraplegia due to SPAST mutations is modified by the  
667 underlying mutation and sex. *Brain* **141**, 3331-3342 (2018).
- 668 60. Solowska, J.M., Rao, A.N. & Baas, P.W. Truncating mutations of SPAST  
669 associated with hereditary spastic paraplegia indicate greater accumulation and  
670 toxicity of the M1 isoform of spastin. *Mol. Biol. Cell* **28**, 1728-1737 (2017).
- 671 61. Ji, Z. *et al.* Spastin interacts with CRMP5 to promote neurite outgrowth by  
672 controlling the microtubule dynamics. *Dev. Neurobiol.* **78**, 1191-1205 (2018).
- 673 62. Gao, Y. *et al.* Atlastin-1 regulates dendritic morphogenesis in mouse cerebral  
674 cortex. *Neurosci. Res.* **77**, 137-142 (2013).
- 675 63. Romeo, D.M. *et al.* Sex differences in cerebral palsy on neuromotor outcome: a  
676 critical review. *Dev. Med. Child Neurol.* **58**, 809-813 (2016).
- 677 64. Reid, S.M., Meehan, E.M., Arnup, S.J. & Reddihough, D.S. Intellectual disability  
678 in cerebral palsy: a population-based retrospective study. *Dev. Med. Child*  
679 *Neurol.* **60**, 687-694 (2018).
- 680 65. Pinero, J. *et al.* DisGeNET: a comprehensive platform integrating information on  
681 human disease-associated genes and variants. *Nucleic Acids Res.* **45**, D833-  
682 D839 (2017).
- 683 66. Szklarczyk, D. *et al.* STRING v11: protein-protein association networks with  
684 increased coverage, supporting functional discovery in genome-wide  
685 experimental datasets. *Nucleic Acids Res.* **47**, D607-D613 (2019).
- 686 67. Al-Mubarak, B. *et al.* Whole exome sequencing reveals inherited and de novo  
687 variants in autism spectrum disorder: a trio study from Saudi families. *Sci. Rep.*  
688 **7**, 5679 (2017).
- 689 68. Giacomuzzi, E. *et al.* Exome sequencing in schizophrenic patients with high levels  
690 of homozygosity identifies novel and extremely rare mutations in the  
691 GABA/glutamatergic pathways. *PLoS One* **12**, e0182778 (2017).
- 692 69. Huang da, W., Sherman, B.T. & Lempicki, R.A. Systematic and integrative  
693 analysis of large gene lists using DAVID bioinformatics resources. *Nat. Protoc.* **4**,  
694 44-57 (2009).
- 695 70. Liberzon, A. *et al.* The Molecular Signatures Database (MSigDB) hallmark gene  
696 set collection. *Cell Syst.* **1**, 417-425 (2015).
- 697 71. Mi, H. *et al.* Protocol Update for large-scale genome and gene function analysis  
698 with the PANTHER classification system (v.14.0). *Nat. Protoc.* **14**, 703-721  
699 (2019).
- 700 72. Fang, H. & Gough, J. DcGO: database of domain-centric ontologies on functions,  
701 phenotypes, diseases and more. *Nucleic Acids Res.* **41**, D536-D544 (2013).
- 702 73. Novarino, G. *et al.* Exome sequencing links corticospinal motor neuron disease  
703 to common neurodegenerative disorders. *Science* **343**, 506-511 (2014).
- 704 74. Stessman, H.A. *et al.* Targeted sequencing identifies 91 neurodevelopmental-  
705 disorder risk genes with autism and developmental-disability biases. *Nat. Genet.*  
706 **49**, 515-526 (2017).

707 75. Estes, P.S. *et al.* Wild-type and A315T mutant TDP-43 exert differential  
708 neurotoxicity in a Drosophila model of ALS. *Hum. Mol. Genet.* **20**, 2308-2321  
709 (2011).

710 76. Madabattula, S.T. *et al.* Quantitative analysis of climbing defects in a Drosophila  
711 model of neurodegenerative disorders. *J. Vis. Exp.*, e52741 (2015).

712 77. Kim, M. *et al.* Mutation in ATG5 reduces autophagy and leads to ataxia with  
713 developmental delay. *Elife* **5**, e12245 (2016).

714 78. Aleman-Meza, B., Loeza-Cabrera, M., Pena-Ramos, O., Stern, M. & Zhong, W.  
715 High-content behavioral profiling reveals neuronal genetic network modulating  
716 Drosophila larval locomotor program. *BMC Genet.* **18**, 40 (2017).

717 79. Hemminki, K., Li, X., Sundquist, K. & Sundquist, J. High familial risks for cerebral  
718 palsy implicate partial heritable aetiology. *Paediatr. Perinat. Epidemiol.* **21**, 235-  
719 241 (2007).

720 80. MacLennan, A.H. *et al.* Cerebral palsy and genomics: an international  
721 consortium. *Dev. Med. Child Neurol.* **60**, 209-210 (2018).

722 81. Himmelmann, K. & Uvebrant, P. The panorama of cerebral palsy in Sweden part  
723 XII shows that patterns changed in the birth years 2007-2010. *Acta Paediatr.*  
724 **107**, 462-468 (2018).

725 82. van Eyk, C.L. *et al.* Analysis of 182 cerebral palsy transcriptomes points to  
726 dysregulation of trophic signalling pathways and overlap with autism. *Transl.*  
727 *Psychiatry* **8**, 88 (2018).

728 83. Martinelli, S. *et al.* Functional dysregulation of CDC42 causes diverse  
729 developmental phenotypes. *Am. J. Hum. Genet.* **102**, 309-320 (2018).

730 84. Englander, Z.A. *et al.* Brain structural connectivity increases concurrent with  
731 functional improvement: evidence from diffusion tensor MRI in children with  
732 cerebral palsy during therapy. *Neuroimage Clin.* **7**, 315-324 (2015).

733 85. Loubet, D. *et al.* Neuritogenesis: the prion protein controls beta1 integrin  
734 signaling activity. *FASEB J.* **26**, 678-690 (2012).

735 86. Colombo, S. *et al.* G protein-coupled potassium channels implicated in mouse  
736 and cellular models of GNB1 encephalopathy. *bioRxiv*, 697235 (2019).

737 87. Pipo-Deveza, J. *et al.* Rationale for dopa-responsive CTNNB1/ $\beta$ -catenin deficient  
738 dystonia. *Mov. Disord.* **33**, 656-657 (2018).

739 88. Akizu, N. *et al.* AMPD2 regulates GTP synthesis and is mutated in a potentially  
740 treatable neurodegenerative brainstem disorder. *Cell* **154**, 505-517 (2013).

741  
742  
743

744 **FIGURE LEGENDS**

745

746 **Figure 1 | Functional validation of CP-associated RHOB variant S73F.** **a**, Sanger  
747 traces of mother, father, and proband from families F064 and F244 verifies *de novo*  
748 inheritance and position of variant (red arrow). **b**, Poisson-Boltzman electrostatic map of  
749 wild-type RHOB (left) and F73 variant (right) showing changes to the kinase binding site  
750 (arrow) and surface charge of the protein. Alignment between human Rho-family  
751 proteins shows high conservation of the RhoB 73 residue in the Switch II domain. The  
752 site of S73/F73 has been labeled (arrow). **c**, Brain MRI from F064 demonstrates  
753 bilateral periventricular T2/FLAIR hyperintensity (arrows) on axial imaging, while sagittal  
754 views reveals equivocal thinning of the isthmus of the corpus callosum (star). MRI from  
755 F244 T2 hyperintensity of posterior limb of internal capsule and optic radiations (left)  
756 and hyperintensity of periventricular white matter (right). **d**, GTP hydrolysis is enhanced  
757 ~1.5-fold in the S73F RHOB variant in a GTPase activating protein (GAP) assay.  
758 Absorbance measurements of hydrolyzed GTP in the presence of either low (5 µg) ( $P =$   
759  $0.003$ ) or high (13 µg) ( $P = 5.6 \times 10^{-5}$ ) RhoA GAP. There was no change in endogenous  
760 GTPase activity with S73F variant without added GAP added (not shown) ( $n = 3$ ). **e**,  
761 GTP binding is enhanced in the S73F RHOB variant in a guanine exchange factor  
762 (GEF) assay. The N-methylantraniloyl-GFP fluorophore increases its fluorescence  
763 emission when bound to Rho-family GTPases, indicating nucleotide uptake by the  
764 GTPase. Both wild-type and S73F have low endogenous GTP binding (lower curves). In  
765 the presence of the Dbs GEF protein, GTP binding is enhanced, and S73F  $K_m$  is  
766 significantly reduced compared to wild-type RHOB ( $n = 5$ ) (mean 243 vs. 547 seconds,  
767  $P = 0.0017$ ). **f**, S73F GTP-binding is increased 4-fold in a pull-down assay with  
768 Rhotekin, an interactor with active GTP-bound Rho proteins. (Top) Sample western blot  
769 cropped to show RHOB from bead-bound fraction and total input detected using  
770 antibody against V5 tag. (Bottom) Quantification of ratio of rhotekin-bound/total RHOB  
771 ( $n = 5$ ),  $P = 0.001$ . Bars in **f** indicate standard error. RFU, relative fluorescence units  
772 ( $10^6$ ) at 360 nm excitation. Statistics determined by two-tailed unpaired *t*-test.  $**P <$   
773  $0.003$ . Full-length blots are provided as **Source Data Figure 1**.

774

775 **Figure 2 | Functional validation of CP-associated FBXO31 variant D334N shows**  
776 **alterations in cyclin D regulation.** **a**, Sanger traces of mother, father, and proband  
777 from families F218 and F699 verifies *de novo* inheritance and position of variant (red  
778 arrow). **b**, Poisson-Boltzman electrostatic map of wild-type FBXO31 (left) and the  
779 D334N variant (right). D334 is positioned around the cyclin D1 (green) binding pocket  
780 on FBXO31. The mutation alters the surface electrostatic charge around the cyclin D1  
781 binding site with a predicted effect on cyclin D1 binding to FBXO31. The site of  
782 D334/D334N has been labeled (arrow). Magnified view of showing alterations to surface  
783 charge in cyclin D1 binding site shown below. **c**, Representative western blot cropped to  
784 show decreased cyclin D expression in patient-derived fibroblasts with *FBXO31*  
785 p.D334N variant. Quantification of Cyclin D is normalized to in-lane  $\beta$ -tubulin and within-  
786 experiment control GMO8398. Both patients had reduced cyclin D compared to pooled  
787 controls. Data averaged for three independent cell culture experiments ( $n = 7$  controls,  $n$   
788  $= 6$  patient measurements). Box indicates 75<sup>th</sup> and 25<sup>th</sup> percentile with median line;

789 whiskers indicate 10<sup>th</sup> and 90<sup>th</sup> percentile. \*\* $P = 0.004$  calculated using two-tailed  
790 unpaired  $t$ -test. Full-length blots are provided as **Source Data Figure 2**.

791  
792 **Figure 3 | Genetic overlap between common neurodevelopmental disorders. a,**  
793 Venn diagram showing number of overlapping genes between candidate cerebral palsy  
794 (CP) genes and genes linked to other neurodevelopmental disorders (NDDs) intellectual  
795 disability (ID), epilepsy, and autism spectrum disorder (ASD). CP risk genes were  
796 identified as having one or more damaging variant across modes of inheritance with  
797 overlap determined using DisGeNET. **b,** Overlap between CP and other NDDs was  
798 significant by hypergeometric two-tailed test, while overlap between CP and Alzheimer's  
799 disease was not. Total number of genes in DisGeNET = 17,549; total number of genes  
800 in our gene set = 439.

801  
802 **Figure 4 | Locomotor phenotypes of loss of function mutations in Drosophila**  
803 **orthologs of candidate cerebral palsy risk genes. a,** Turning time, a measure of  
804 coordinated movements, is increased in larvae with mutations in *AGAP1*, *SEMA4A*, and  
805 *TENM1* orthologs. Drosophila mutant and control genotypes are provided in  
806 **Supplementary Table 9. b-i,** 14 day-old adult flies have locomotor impairments. **b-e,**  
807 Negative geotaxis climbing defects in distance threshold assay for flies with mutations in  
808 orthologs of *DOCK11* (**b**), *RABEP1* (**c**), *PTK2B* (**d**) and *ATL1* (**e**). Some genotypes have  
809 a male-specific locomotor defect (**c**). **f-g,** Increased number of falls for flies with  
810 mutations in *SYNGAP1* (**f**) and *TBC1D17* (**g**) orthologs, although % reaching threshold  
811 distance was normal (**Extended Data Fig. 10**). **h-i,** Impairments in the average distance  
812 traveled of flies with mutations in *MKL1* (**h**) and *ZDHHC15* (**i**) orthologs. Related GO  
813 terms for genes are shown in bold. For box and whisker plots, box indicates 75<sup>th</sup> and  
814 25<sup>th</sup> percentile with median line, and whiskers indicate 10<sup>th</sup> and 90<sup>th</sup> percentile.  
815 Locomotor curve represents average of all trials and bars indicate standard error.  $n = 50$   
816 larvae,  $n = 10-21$  trials for falls and distance traveled assays, and  $n = 10-21$  trials for  
817 locomotor curves. Difference between larval turning time, distance traveled, and number  
818 of falls determined by unpaired two-tailed  $t$ -test. Locomotor curves were considered to  
819 be significantly different from each other if  $P < 0.05$  for Kolomogrov-Smirnov test in  
820 addition to a significant difference at one or 1 or more time bins by Mann-Whitney rank  
821 sum two-tailed test. \* $P < 0.05$ , \*\* $P < 0.005$ , \*\*\* $P < 0.001$ , \*\*\*\* $P < 1 \times 10^{-6}$ . Exact  
822 genotypes,  $n$ , and  $P$  values are provided in **Supplementary Table 9. j,** Enrichment of  
823 locomotor phenotypes detected in studies of putative CP genes (observed) compared to  
824 genome-wide rates annotated in Flybase.org (expected, 3.1%).  $P$  value was calculated  
825 by Fisher's exact two-tailed test.

826  
827  
828  
829  
830  
831

832 **TABLES**

833

834 **Table 1 | Significant enrichment of DNMs in CP cases.** A one-tailed Poisson test was  
 835 used to test the enrichment of DNMs for each functional class. A marginal enrichment of  
 836 DNMs was observed for loss-of-function (LoF), protein-altering, and damaging DNMs.  
 837 Strikingly, when we restricted our analysis to LoF-intolerant genes, stronger enrichment  
 838 was observed for protein-altering and damaging DNMs, suggesting a significant  
 839 contribution of DNM in this gene set to CP pathogenesis. No enrichment was found in  
 840 controls. *n*, number of DNMs; rate, number of DNMs divided by the number of  
 841 individuals in the cohort; enrichment, ratio of observed to expected numbers of  
 842 mutations; D-Mis, damaging missense mutations as predicted by MetaSVM and CADD  
 843 algorithms; Protein-altering, missense + LoF; Damaging, D-Mis + LoF.  
 844

	Cases, <i>n</i> = 250						Controls, <i>n</i> = 1,789						
	Observed		Expected		Enrichment	<i>P</i>	Observed		Expected		Enrichment	<i>P</i>	
	<i>n</i>	Rate	<i>n</i>	Rate			<i>n</i>	Rate	<i>n</i>	Rate			
<b>All genes (<i>n</i> = 19,347)</b>							<b>All genes (<i>n</i> = 19,347)</b>						
Total	298	1.19	276.8	1.11	1.08	0.11	Total	1,834	1.03	1,967.2	1.10	0.93	1.00
Synonymous	68	0.27	78.4	0.31	0.87	0.89	Synonymous	484	0.27	557	0.31	0.87	1.00
T-Mis	63	0.25	61.3	0.25	1.03	0.43	T-Mis	410	0.23	431.6	0.24	0.95	0.86
D-Mis	132	0.53	113.1	0.45	1.17	0.04	D-Mis	790	0.44	808.1	0.45	0.98	0.74
LoF	35	0.14	24.1	0.10	1.46	0.02	LoF	150	0.08	170.4	0.10	0.88	0.95
Protein-altering	230	0.92	198.5	0.79	1.16	0.02	Protein-altering	1,350	0.75	1,410.2	0.79	0.96	0.95
Damaging	167	0.67	137.2	0.55	1.22	$7.4 \times 10^{-3}$	Damaging	940	0.53	978.5	0.55	0.96	0.89
<b>Loss-of-function intolerant genes (gnomADv2.1.1 pLI <math>\geq</math> 0.9; <i>n</i> = 3,049)</b>							<b>Loss-of-function intolerant genes (gnomADv2.1.1 pLI <math>\geq</math> 0.9; <i>n</i> = 3,049)</b>						
Total	99	0.40	66.4	0.27	1.49	$1.1 \times 10^{-4}$	Total	456	0.25	473.8	0.26	0.96	0.80
Synonymous	20	0.08	18.7	0.07	1.07	0.41	Synonymous	113	0.06	133.4	0.07	0.85	0.97
T-Mis	13	0.05	10.7	0.04	1.21	0.28	T-Mis	86	0.05	75.5	0.04	1.14	0.13
D-Mis	53	0.21	31.1	0.12	1.70	$2.3 \times 10^{-4}$	D-Mis	222	0.12	222.7	0.12	1.00	0.53
LoF	13	0.05	5.9	0.02	2.19	$8.1 \times 10^{-3}$	LoF	35	0.02	42.2	0.02	0.83	0.89
Protein-altering	79	0.32	47.7	0.19	1.66	$2.1 \times 10^{-5}$	Protein-altering	343	0.19	340.4	0.19	1.01	0.45
Damaging	66	0.26	37.1	0.15	1.78	$1.2 \times 10^{-5}$	Damaging	257	0.14	264.9	0.15	0.97	0.69

845

846

847 **Table 2 | Eight genes with two or more damaging (LoF + D-Mis) DNMs.** A one-tailed  
 848 Poisson-test was performed for damaging and LoF DNMs for each gene independently.  
 849 The Bonferroni correction for genome-wide significance is  $1.3 \times 10^{-6}$  (= 0.05/(19,347  
 850 genes x 2 tests)).  
 851

Gene	# LoF	# D-Mis	Poisson P-value	pLI	mis_Z
<b>CTNNB1</b>	<b>3</b>	<b>0</b>	<b><math>9.8 \times 10^{-10}</math></b>	<b>1.00</b>	<b>3.85</b>
<b>TUBA1A</b>	<b>0</b>	<b>3</b>	<b><math>4.8 \times 10^{-8}</math></b>	<b>0.97</b>	<b>5.58</b>
<i>RHOB</i>	0	2	$7.6 \times 10^{-6}$	0.12	2.51
<i>ATL1</i>	0	2	$2.0 \times 10^{-5}$	0.98	2.63
<i>DHX32</i>	0	2	$3.5 \times 10^{-5}$	0.00	1.26
<i>SPAST</i>	0	2	$3.5 \times 10^{-5}$	1.00	1.24
<i>FBXO31</i>	0	2	$5.1 \times 10^{-5}$	0.44	2.46
<i>ALK</i>	1	1	$2.5 \times 10^{-4}$	0.00	0.01

852  
 853

854 **Table 3 | Idiopathic CP cases show enrichment of damaging recessive genotypes**  
855 **(RGs) in HSP-associated genes.** One-tailed binomial test coupled with the polynomial  
856 regression model was conducted to evaluate the enrichment of damaging RGs in known  
857 HSP-associated genes in cases and in controls, respectively. Stratified analysis by the  
858 diagnosis of CP shows that the enrichment of these damaging RGs was specific to  
859 cryptogenic cases. Multiple-testing  $P$ -value cutoff was  $6.3 \times 10^{-3}$  ( $= 0.05/(2 \times 4)$ ).  
860

Gene set (# genes)	Observed				Expected Recessive genotypes	Enrichment	$P$
	Homozygotes	Compound heterozygous	Unique genes	Recessive genotypes			
<b>250 CP cases</b>							
All genes (19,347)	63	133	187	196	-	-	-
Recessive known HSP genes (52)	3	3	6	6	0.78	<b>7.74</b>	<b><math>1.5 \times 10^{-4}</math></b>
Known HSP genes (73)	3	3	6	6	0.97	<b>6.20</b>	<b><math>4.8 \times 10^{-4}</math></b>
<b>157 idiopathic cases</b>							
All genes (19,347)	49	89	136	138	-	-	-
Recessive known HSP genes (52)	3	2	5	5	0.54	<b>9.22</b>	<b><math>2.4 \times 10^{-4}</math></b>
Known HSP genes (73)	3	2	5	5	0.68	<b>7.37</b>	<b><math>6.5 \times 10^{-4}</math></b>
<b>84 environmental cases</b>							
All genes (19,347)	14	41	40	55	-	-	-
Recessive known HSP genes (52)	0	1	1	1	0.22	4.48	0.20
Known HSP genes (73)	0	1	1	1	0.28	3.60	0.24
<b>1,789 controls</b>							
All genes (19,347)	81	687	610	768	-	-	-
Recessive known HSP genes (52)	0	3	3	3	2.46	1.22	0.45
Known HSP genes (73)	0	3	3	3	2.94	1.02	0.56

861

862



863 **Table 4 | CP risk gene pathway enrichment.** Key pathways and terms overlapping  
864 between DAVID, PANTHER, and MSigDB bioinformatics tools. Gene ontology (GO)  
865 terms include cell projections, cytoskeleton, and Rho GTPase signaling. GO terms were  
866 extracted from the total set (**Supplementary Data Sets 6-15**) using hierarchical nesting,  
867 or functions that were represented by multiple GO terms. Overlap/Set refers to number  
868 of genes overlapping between CP risk gene and Database/Number of genes in  
869 Database for that term. FDR =  $q$  value (false discovery rate cutoff = 0.05) from two-  
870 tailed Fisher and hypergeometric tests. FDR differences are due to differences in tool  
871 methodologies.

Database	Terms	Overlap/Set	Observed	Expected	FDR
DAVID	Non-integrin membrane-ECM interactions (R-HSA-3000171)	10/40	10/218	40/9075	0.00045
	Laminin interactions(R-HSA-3000157)	8/30	8/218	30/9075	0.0075
	ECM-receptor interaction (R-HSA-04512)	12/87	12/168	87/6879	0.00888
PANTHER	Non-integrin membrane-ECM interactions (R-HSA-3000171)	12/59	12/447	59/20851	6.02x10 <sup>-5</sup>
	Laminin interactions (R-HSA-3000157)	8/30	8/447	30/20851	0.00114
	Signaling by Rho GTPases (R-HSA-194315)	24/408	24/447	408/20851	0.00721
	Extracellular matrix organization (R-HSA-1474244)	20/299	20/447	299/20851	0.00826
MSigDB	Non-integrin membrane-ECM interactions (R-HSA-30000171)	12/59	12/439	59/38055	5.53x10 <sup>-9</sup>
	Laminin interactions (R-HSA-30000157)	8/30	8/439	30/38055	4.65x10 <sup>-7</sup>
	Signaling by Rho GTPases (R-HSA-194315)	26/450	26/439	450/38055	2.15x10 <sup>-8</sup>
	Extracellular matrix organization (R-HSA-1474244)	20/301	20/439	301/38055	1.97x10 <sup>-7</sup>
<b>Biological processes</b>	<b>Cell projection and organization</b>				
	Regulation of cell projection organization (GO:0031344)	47/695	47/447	695/20851	1.35x10 <sup>-7</sup>
	Positive regulation of cell projection organization (GO:0031346)	30/395	30/447	395/20851	1.84x10 <sup>-5</sup>
	Positive regulation of neuron projection development (GO:0010976)	19/294	19/447	294/20851	0.0087
	<b>Microtubule based movement</b>				
	Movement of cell or subcellular component (GO:0006928)	66/1544	66/447	1544/20851	1.22x10 <sup>-4</sup>
	Microtubule-based process (GO:0007017)	32/667	32/447	667/20851	0.00875
Microtubule-based movement (GO:0007018)	18/271	18/447	271/20851	0.00966	
<b>Cell components</b>	<b>Axonal cell projection</b>				
	Plasma membrane bounded cell projection part (GO:0120025)	89/2197	89/447	2197/20851	7.15x10 <sup>-6</sup>
	Axon (GO:0030424)	34/641	34/447	641/20851	0.000882
	Actin-based cell projection (GO:0098858)	15/214	15/447	214/20851	0.00898
	<b>Microtubule associated components</b>				
	Cytoskeleton (GO:0005856)	82/2274	82/447	2274/20851	0.000894
	Microtubule cytoskeleton (GO:0015630)	46/1246	46/447	1246/20851	0.0213
Microtubule associated complex (GO:0005875)	11/154	11/447	154/20851	0.0302	
<b>Molecular functions</b>	<b>GTPase activity</b>				
	Small GTPase binding (GO:0031267)	28/421	28/421	421/20851	7.98x10 <sup>-5</sup>
	Rho GTPase binding (GO:0017048)	19/145	19/447	145/20851	9.63x10 <sup>-7</sup>
	GTPase regulator activity (GO:0030695)	18/307	18/447	307/20851	0.0211
	<b>Actin cytoskeleton regulation</b>				
	Extracellular matrix structural constituent (GO:0005201)	15/165	15/447	165/20851	0.00108
Actin binding (GO:0003779)	23/443	23/447	443/20851	0.0207	

873

874 **METHODS**

875

876 **Case cohorts, enrollment, phenotyping, and exclusion criteria.** 159 CP cases (132  
877 idiopathic, 24 environmental, 3 unclassified) and their unaffected parents were recruited  
878 via Phoenix Children’s Hospital, the University of Adelaide, and Zhengzhou City  
879 Children’s Hospital. Six of these were recently published as part of a gene panel  
880 study<sup>89</sup>. Exclusion criteria and detailed descriptions about these cohorts are provided  
881 separately below. Further, 91 previously published<sup>22</sup> trios (25 idiopathic, 60  
882 environmental, 6 unknown) were included to allow for comparison of idiopathic and  
883 environmental subtypes of CP.

884

885 **CP classification.** CP cases were subdivided into idiopathic, environmental, and  
886 unclassified groups based upon data available at the time of ascertainment. This  
887 designation was revised as appropriate as additional data became available. Cases  
888 were designated “environmental” if any idiopathic exclusion criteria were met.

889

890 **Exclusion criteria for idiopathic status.** Potential participants were excluded from an  
891 “idiopathic” designation if any of the following were present: prematurity (estimated  
892 gestational age < 32 weeks), stroke, intraventricular hemorrhage, major brain  
893 malformation (i.e. lissencephaly, pachygyria, polymicrogyria, schizencephaly, simplified  
894 gyri, brainstem dysgenesis, cerebellar hypoplasia, etc.), hypoxic-ischemic injury (as  
895 defined by treating physicians), *in utero* infection, hydrocephalus, traumatic brain injury,  
896 respiratory arrest, cardiac arrest, or brain calcifications. The following did not  
897 automatically indicate environmental status even if parents believed this was the cause  
898 of the child’s CP: history of prematurity (but delivery at greater than or equal to 32  
899 weeks gestational age), nuchal cord, difficult delivery, fetal decelerations, urgent C-  
900 section, preterm bleeding, or maternal infection. In equivocal cases, additional data was  
901 sought until a decision regarding group assignment could be made by the  
902 corresponding author. Periventricular leukomalacia was not considered universally  
903 indicative of environmental status<sup>90</sup>.

904

905 **Movement disorder, pattern of involvement, and functional status.** Spasticity,  
906 dystonia, chorea/athetosis, ballism, hypotonia, and/or ataxia were assessed by the  
907 treating specialist, who also assigned Gross Motor Functional Classification System  
908 scores as well as the pattern of involvement.

909 *Phoenix Children’s Hospital (PCH; n = 52).* Patients with CP according to  
910 international consensus criteria<sup>23</sup> were recruited from CP subspecialty clinics (pediatric  
911 movement disorders neurology, pediatric orthopedics, pediatric neurosurgery, pediatric  
912 physiatry) at PCH or the clinics of collaborators at outside institutions using a local  
913 ethics-approved protocol or a PCH-approved central IRB protocol (#15-080). Written  
914 informed consents were obtained for parents and assent was obtained for children as  
915 appropriate for families wishing to participate. Blood, buccal swab and/or saliva samples  
916 were collected from the affected child and both parents. DNA was extracted with the  
917 support of the PCH Biorepository using a Kingfisher Automated Extraction System™,  
918 and quality control metrics, including yield, 260/280, and 260/230 ratio were recorded.

919 *University of Adelaide Robinson Research Institute (n = 63)*. Ethics permission was  
920 obtained in each state and overall from the Adelaide Women's and Children's Health  
921 Network Human Research Ethics Committee South Australia. Families were enrolled  
922 from among children attending major children's hospitals in South Australia, New South  
923 Wales and Queensland where a diagnosis of CP had been confirmed by a specialist in  
924 pediatric rehabilitation according to international consensus criteria<sup>23</sup>. Blood for DNA  
925 from cases was collected under general anaesthesia during procedures such as Botox  
926 injections or orthopedic surgery and parental blood collected whenever possible.  
927 Lymphoblastoid cell lines (LCLs) were generated for each case at Genetic Repositories  
928 Australia.

929 *Zhengzhou City Children's Hospital (n = 44)*. This study was approved after  
930 review by the ethics committee of Zhengzhou City Children's Hospital. Parent-offspring  
931 trios were recruited from children with CP without apparent cause at Zhengzhou City  
932 Children's Hospital. Cases were additionally excluded if intrauterine growth retardation,  
933 threatened pre-term birth, premature rupture of membranes, pregnancy-induced  
934 hypertension, or multiple births was present. All participants and their guardians  
935 provided written informed consent under the auspices of the local ethics board. DNA  
936 was extracted from blood samples using standard methods.

937  
938 **Control cohorts.** Controls consisted of 1,789 previously sequenced families that  
939 included one child with autism, one unaffected sibling, and the unaffected parents<sup>25</sup>. For  
940 use in this study, only the unaffected sibling and parents were analyzed. Controls were  
941 designated as unaffected by the Simons Simplex Collection (SSC). Permission to  
942 access the genomic data in the SSC via the National Institute of Mental Health Data  
943 Repository was obtained. Written informed consent for all participants was provided by  
944 the Simons Foundation Autism Research Initiative.

945  
946 **Exome sequencing.** Most trios were sequenced at the Yale Center for Genome  
947 Analysis following an identical protocol (**Supplementary Table 2**). Briefly, genomic  
948 DNA from venous blood, buccal swabs, saliva, or LCL lines (Adelaide) was captured  
949 using the Nimblegen SeqxCap EZ MedExome Target Enrichment Kit (Roche) or the  
950 xGEN Exome Research Panel v1.0 (IDT) followed by Illumina DNA sequencing as  
951 previously described<sup>24</sup>. Trio samples from Zhengzhou were prepared using Exome  
952 Library Prep kits (Illumina), followed by Illumina sequencing. Eight trios from Adelaide  
953 sequenced at the University of Washington were prepared using the SureSelect Human  
954 All Exon V5 (Agilent) and underwent Illumina sequencing. One trio sequenced by  
955 GeneDx was captured using the Agilent SureSelect Human All Exon V4 while one trio  
956 sequenced by the Hôpital Pitié-Salpêtrière used the Roche MedExome capture kit, in  
957 both cases followed by Illumina sequencing. Ninety-one previously published trios from  
958 Adelaide were captured using the VCRome 2.1 kit (HGSC), followed by Illumina  
959 sequencing as described previously<sup>22</sup> (**Supplementary Data Set 1**). Sequencing  
960 metrics suggest that, regardless of the exome capture reagent used, all samples had  
961 sufficient sequencing coverage to make confident variant calls with a mean coverage of  
962  $\geq 46\times$  at each targeted base and more than 90% of targeted bases with  $\geq 8$  independent  
963 reads.

964

965 **Mapping and variant calling.** WES data were processed using two independent  
966 pipelines at the Yale School of Medicine and PCH. At each site, sequence reads were  
967 independently mapped to the reference genome (GRCh37) with BWA-MEM and further  
968 processed using GATK Best Practice workflows, which include duplication marking,  
969 indel realignment, and base quality recalibration, as previously described<sup>26,27,91</sup>. Single  
970 nucleotide variants and small indels were called with GATK HaplotypeCaller and  
971 annotated using ANNOVAR<sup>92</sup>, dbSNP (v138), 1000 Genomes (August 2015), NHLBI  
972 Exome Variant Server (EVS), and the Exome Aggregation Consortium v3 (ExAC)<sup>93</sup>.  
973 MetaSVM and Combined Annotation Dependent Deletion (CADD v1.3) algorithms were  
974 used to predict deleteriousness of missense variants (“D-Mis”, defined as MetaSVM-  
975 deleterious or CADD  $\geq 20$ )<sup>28,29</sup>. Inferred LoF variants consist of stop-gain, stop-loss,  
976 frameshift insertions/deletions, canonical splice site, and start-loss. LoF + D-Mis  
977 mutations were considered “damaging”. Variant calls were reconciled between Yale and  
978 PCH prior to downstream statistical analyses. Variants were considered by mode of  
979 inheritance, including DNMs, RGs, and X-linked variants. Protein annotations in  
980 **Extended Data Figures 3-8** were obtained using Geneious Prime 2020.0.5.  
981 (<https://www.geneious.com>).  
982

983 **Variant filtering.** DNMs were called using the TrioDenovo<sup>30</sup> program by Yale and PCH  
984 separately as described previously<sup>24</sup>, and filtered using stringent hard cutoffs. These  
985 hard filters include: (i) MAF  $\leq 4 \times 10^{-4}$  in ExAC; (ii) a minimum 10 total reads total, 5  
986 alternate allele reads, and a minimum 20% alternate allele ratio in the proband if  
987 alternate allele reads  $\geq 10$  or, if alternate allele reads is  $< 10$ , a minimum 28% alternate  
988 ratio; (iii) a minimum depth of 10 reference reads and alternate allele ratio  $< 3.5\%$  in  
989 parents; and (iv) exonic or canonical splice-site variants.

990 For the X-linked hemizygous variants, we filtered for rarity (MAF  $\leq 5 \times 10^{-5}$  across  
991 all samples in 1000 Genomes, EVS, and ExAC) and high-quality heterozygotes (pass  
992 GATK Variant Score Quality Recalibration (VSQR), minimum 8 total reads, genotype  
993 quality (GQ) score  $\geq 20$ , mapping quality (MQ) score  $\geq 40$ , and minimum 20% alternate  
994 allele ratio in the proband if alternate allele reads  $\geq 10$  or, if alternate allele reads is  $<$   
995 10, a minimum 28% alternate ratio)<sup>93,94</sup>. Additionally, variants located in segmental  
996 duplication regions (as annotated by ANNOVAR<sup>28</sup>), RGs, and DNMs were excluded.  
997 Finally, *in silico* visualization was performed on: (i) variants that appear at least twice  
998 and (ii) variants in the top 20 significant genes from the analysis.

999 We filtered RGs for rare (MAF  $\leq 10^{-3}$  across all samples in 1000 Genomes, EVS,  
1000 and ExAC) homozygous and compound heterozygous variants that exhibited high  
1001 quality sequence reads (pass GATK VSQR) and had a minimum 8 total reads total for  
1002 proband. Only LoF variants (stop-gain, stop-loss, canonical splice-site, frameshift indels,  
1003 and start-loss), D-Mis (MetaSVM = D or CADD  $\geq 20$ ), and non-frameshift indels were  
1004 considered potentially damaging to protein function.  
1005

1006 **Estimation of expected number of RGs.** We implemented a multivariate regression  
1007 model to quantify the enrichment of damaging RGs in a specific gene or gene set in  
1008 cases, independent of controls. Additional details about the modeling of the distribution  
1009 of RG counts are described in our recent study<sup>24</sup>.  
1010

1011 **Statistical analysis. *De novo enrichment analysis.*** The R package ‘denovolyzeR’ was  
 1012 used for the analysis of DNMs based on a mutation model developed previously<sup>95</sup>. The  
 1013 probability of observing a DNM in each gene was derived as described previously<sup>96</sup>,  
 1014 except that the coverage adjustment factor was based on the full set of 250 case trios or  
 1015 1,789 control trios (separate probability tables for each cohort). The overall enrichment  
 1016 was calculated by comparing the observed number of DNMs across each functional  
 1017 class to expected under the null mutation model. The expected number of DNMs was  
 1018 calculated by taking the sum of each functional class specific probability multiplied by  
 1019 the number of probands in the study, multiplied by two (diploid genomes). The Poisson  
 1020 test was then used to test for enrichment of observed DNMs versus expected as  
 1021 implemented in denovolyzeR<sup>95</sup>. For gene set enrichment, the expected probability was  
 1022 calculated from the probabilities corresponding to the gene set only.

1023 To estimate the number of genes with > 1 DNM, 1 million permutations were  
 1024 performed to derive the empirical distribution of the number of genes with multiple  
 1025 DNMs. For each permutation, the number of DNMs observed in each functional class  
 1026 was randomly distributed across the genome adjusting for gene mutability<sup>24</sup>. The  
 1027 empirical *P*-value was calculated as the proportion of times that the number of recurrent  
 1028 genes from the permutation is greater than or equal to the observed number of  
 1029 recurrent genes.

1030 To examine whether any individual gene contains more DNMs than expected,  
 1031 the expected number of DNMs for each functional class was calculated from the  
 1032 corresponding probability adjusting for cohort size. A one-tailed Poisson test was then  
 1033 used to compare the observed DNMs for each gene versus expected. As separate tests  
 1034 were performed for damaging DNMs and LoF DNMs, the Bonferroni multiple-testing  
 1035 threshold is, therefore, equal to  $1.3 \times 10^{-6}$  ( $0.05/(19,347 \text{ genes} \times 2 \text{ tests})$ ). The most  
 1036 significant *P*-value of the two tests was reported.

1037 ***Gene-set enrichment analysis.*** To test for over representation of damaging RGs  
 1038 in a gene set without controls and correct for consanguinity, a one-sided binomial test  
 1039 coupled with the polynomial regression model was conducted by comparing the  
 1040 observed number of variants to the expected count estimated as described before<sup>24</sup>.  
 1041 Assuming that our exome capture reagent captures *N* genes and the testing gene set  
 1042 contains *M* genes, then the *P*-value of finding *k* variants in this gene set out of a total of  
 1043 *x* variants in the entire exome is given by

$$P = \sum_{i=k}^x \binom{x}{i} (p)^i (1-p)^{n-i}$$

1044  
 1045 where

$$P = \left( \sum_{gene\ set} Expected\ Value_i \right) / \left( \sum_{all\ genes} Expected\ Value_j \right)$$

1046  
 1047 Enrichment was calculated as the observed number of genotypes/variants divided by  
 1048 the expected number of genotypes/variants.

1049 ***Gene-based binomial test.*** A one-tailed binomial test was used to compare the  
 1050 observed number of damaging RGs within each gene to the expected number

1051 estimated using the approach detailed above. Enrichment was calculated as the  
1052 number of observed damaging RGs divided by the expected number of damaging RGs.

1053 *Genetic overlap across neurodevelopmental disorders.* We compared the list of  
1054 439 putative CP risk genes (**Supplementary Data Sets 6-15**) with genes identified in  
1055 other major neurodevelopmental disorders using Disease-Gene Network (DisGeNET,  
1056 updated May 2019)<sup>65</sup>. We first extracted all the genes from DisGeNET that were  
1057 associated with autism spectrum disorder (ASD, CUI: C1510586, 571 genes),  
1058 intellectual disability (ID, CUI: C3714756, 2,502 genes) and Epilepsy (EP, CUI:  
1059 C0014544, 1,176 genes). We used the hypergeometric probability to calculate the  
1060 overlap significance. The hypergeometric distribution formula is given by:  
1061

$$P(X = k) = \frac{\binom{K}{k} \binom{N - K}{n - k}}{\binom{N}{n}}$$

1062 where, K = # genes in DisGeNET associated with the disease,  
1063 k = # genes in overlapping set with that disease,  
1064 N = # total genes in DisGeNET,  
1065 n = # total genes in the observed set  
1066

1067  
1068 A Venn Diagram representing the gene number appearing in more than one list was  
1069 created in R using the 'VennDiagram' package.  
1070

1071 **Pathway analysis.** *STRING protein-protein interaction enrichment.* We used the list of  
1072 439 genes (**Supplementary Data Sets 6-15**) to conduct a protein-protein interaction  
1073 (PPI) enrichment for gene networks. We used STRINGv11 to further study protein  
1074 interaction networks in our set of 439 putative CP risk genes with de novo, X-linked  
1075 recessive or autosomal recessive damaging variants. We used 0.70 (high confidence)  
1076 cutoff to derive these interactions network as described<sup>66</sup>. The network visualization can  
1077 be accessed at:

1078 <https://version-11-0.string-db.org/cgi/network.pl?networkId=sKvp4sjmxO4O>

1079 *Gene set over representation analysis.* We used the list of 439 genes  
1080 (**Supplementary Data Sets 6-15**) for further downstream gene set over representation  
1081 analysis using DAVID v6.8<sup>69,97</sup> (updated October 2016), PANTHER v15.0<sup>98</sup> (updated  
1082 2020-02-14) and MSigDB v7.0<sup>99</sup> (updated August 2019). The background gene list for  
1083 all three tools was their respective pool of all human genes. To measure statistical over  
1084 representation of gene sets in the client set, PANTHER uses a Fisher's exact two-tailed  
1085 test, DAVID uses a modified Fisher's test and MSigDB uses the hypergeometric  
1086 distribution two-tailed test.

1087 DcGO<sup>72</sup> algorithm identifies parent and child nesting GO terms to determine  
1088 hierarchal relationships. We started from the most specific GO terms (fewest genes) to  
1089 identify first-level parents. These terms were used with DcGO to identify terms where  
1090 parent, middle, and child terms were all represented on our list with significant FDR.  
1091 These nested terms were manually curated for **Table 4**.  
1092

1093 **RHOB functional assays.** *GTPase activating protein (GAP) assay.* (Cytoskeleton) 13  
1094 µg of purified wild-type or S73F RhoB protein (Origene) was incubated with 20 µM GTP  
1095 with or without 5 µg or 13 µg of p50 RhoGAP for 30 min at 37 °C, then incubated with  
1096 CytoPhos reagent for 15 min at room temperature. Hydrolyzed GTP was detected at  
1097 650 nm on a SpectraMax paradigm microplate reader as per the manufacturer's  
1098 instructions. Data from three independent biological replicates.

1099 *Guanine exchange factor (GEF) assay.* (Cytoskeleton) 2 µM of purified wild-type  
1100 or S73F RhoB protein (Origene) was incubated with or without 2 µM of the GEF domain  
1101 of the human Dbs protein for 30 min at 20 °C. The fluorescence of N-methylantraniloyl  
1102 GTP-analogue binding was measured every 30 s at 360 nm with the SpectraMax as per  
1103 the manufacturer's instructions. Data from five independent biological replicates.

1104 *Rhotekin assay.* (Cytoskeleton) 50 µg of agarose beads coated with the Rho-  
1105 GTP binding domain (residues 7-89) of the human Rhotekin protein were incubated with  
1106 500 µg of lysate from yeast expressing human RHOB-V5 or the S73F variant under  
1107 gentle agitation for 1 h at 4 °C. Beads pelleted by centrifugation at 2,400 xg (5,000 rpm)  
1108 for 4 min at 4 °C and washed three times in Wash Buffer (25 mM Tris pH 7.5, 30 mM  
1109 MgCl<sub>2</sub>, 40 mM NaCl). Beads were resuspended in Laemmli blue 2X and 40 µg of lysate  
1110 used for western blotting. RhoB was identified with a primary monoclonal anti-V5  
1111 antibody (Thermo Fisher) 1:5,000 in BSA and a secondary goat anti-mouse HRP (GE  
1112 Healthcare) 1:5,000. Data from five independent biological replicates.

1113  
1114 **FBXO31 cyclin D abundance assay.** Three independent, passage-matched control  
1115 fibroblast lines (GMO8398, GMO2987, GMO8399 from the Corriell Institute) and two  
1116 patient primary fibroblasts obtained from each patient via punch biopsies were used.  
1117 Total sample  $n = 7$  controls,  $n = 6$  patient measurements. Plates were seeded at  
1118 600,000 cells/well and cultured in DMEM supplemented with 1 mM sodium pyruvate, 1  
1119 mM glutamine (Gibco) and 10% FBS. Fibroblasts were harvested at confluence with  
1120 RIPA buffer (Thermo Fisher) supplemented with protease cocktail (Fischer Scientific) on  
1121 ice and centrifuged. Western blotting was conducted using 10 µg protein/lane with  
1122 antibodies against cyclin D (rabbit polyclonal; ab134175) 1:1,000, β-tubulin (rabbit  
1123 polyclonal, ab6046) 1:5,000 in 5% BSA and detected with anti-rabbit HRP (GE Health  
1124 Sciences) 1:5,000. Signal was quantified using Image Studio Lite and the ratio of cyclin  
1125 D/β-tubulin was normalized to within-experimental control GMO8398. The difference in  
1126 cyclin D abundance was determined using an unpaired *t*-test.

1127  
1128 **Drosophila locomotor experiments.** *Fly rearing and genetics.* Drosophila were reared  
1129 on a standard cornmeal, yeast, sucrose food from the BIO5 media facility, University of  
1130 Arizona. Stocks for experiments were reared at 25 °C, 60-80% relative humidity with  
1131 12:12 light/dark cycle. Cultures for controls and mutants were maintained with the same  
1132 growth conditions, with attention to the density of animals within the vial. Descriptions of  
1133 alleles used for each CP candidate gene can be found in **Supplementary Table 9** and  
1134 included 5' insertional hypomorphs, missense mutations, targeted excision, and  
1135 deficiency chromosomes. Fly stocks were obtained from the Bloomington Drosophila  
1136 Stock Center (NIH P40OD018537) and other investigators. We performed crosses of  
1137 background markers for genetic controls.

1138 *Locomotor assays.* We used naïve, unmated flies collected as pharate adults. To  
1139 minimize variables, we used no anesthesia, and humidity, temperature, and time of day  
1140 were controlled (30-60% RH, 21-23.5 °C, 0900-1200). Flies were adapted to room  
1141 conditions for 1 h before running in groups of 3-20 in a 250 mL graduated cylinder for 2  
1142 min<sup>76</sup>. If <50% crossed the 250 (22.5 cm) mark, flies were re-assayed immediately up to  
1143 three iterations. Flies crossing the 250 mL mark (22.5 cm) were manually scored from  
1144 coded videos in 10-second bins for 10-21 trials/genotype. The number of falls, defined  
1145 as downward movement while detached from the cylinder wall, were manually counted  
1146 and normalized to the number of flies in the recording window per 10-second bin for 10-  
1147 21 trials/genotype. Significant difference of locomotor performance between mutants  
1148 and controls required  $P < 0.05$  for both Kolmogorov-Smirnov test for whole curve and  
1149 Mann-Whitney rank sum test for at least one time bin between 10-30 seconds. Distance  
1150 traveled assay was performed using paired, coded vials of control and mutant flies<sup>77</sup>.  
1151 Distance measured from still image from video at 3 seconds post-tapping using ImageJ  
1152 measure distance function from middle of fly to bottom of vial for 10-11 trials. Larval  
1153 turning time was defined as the amount of time required to turn onto ventral surface and  
1154 initiate forward movement after rotation onto dorsal surface and measured for 50  
1155 larvae/genotype<sup>75</sup>. Significance for vial and larval turning assays were determined using  
1156 *t*-test. Graphs and statistics were performed in R. *Drosophila* locomotor gene  
1157 enrichment analysis performed as described previously<sup>78</sup> using [www.MARRVEL.org](http://www.MARRVEL.org)  
1158 and [www.flybase.org](http://www.flybase.org) to identify the *Drosophila* ortholog and compared to genome-wide  
1159 number of genes identified by the terms locomotor/locomotion, flight, taxis (photo- or  
1160 geo-). Significance of enrichment determined using the Fisher exact two-tailed test.  
1161 Assay validation and additional genetics information is provided in the **Supplementary**  
1162 **Note**.

1163  
1164 **Reporting summary.** Further information on research design is available in the Nature  
1165 Research Reporting Summary linked to this article.

## 1166 1167 1168 **DATA AVAILABILITY STATEMENT**

1169  
1170 Sequencing data from University of Adelaide Robinson Research Institute ( $n = 154$   
1171 trios) are available from the corresponding author on request, subject to human  
1172 research ethics approval and patient consent. Data from Phoenix Children's Hospital ( $n$   
1173 = 52 trios) are available from the corresponding author on request, subject to patient  
1174 consent. Data from Zhengzhou City Children's Hospital ( $n = 44$  trios) are available in the  
1175 CNSA of China National GeneBank DataBase repository (<https://db.cngb.org/cnsa/>).

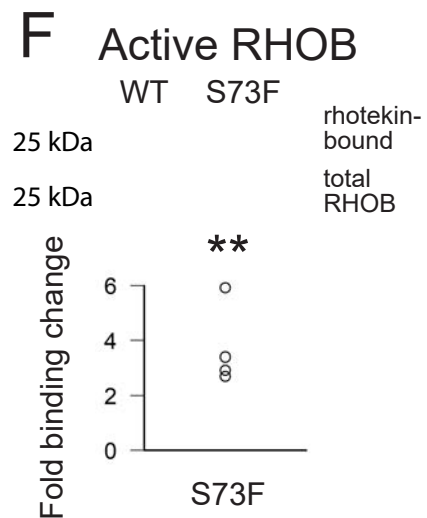
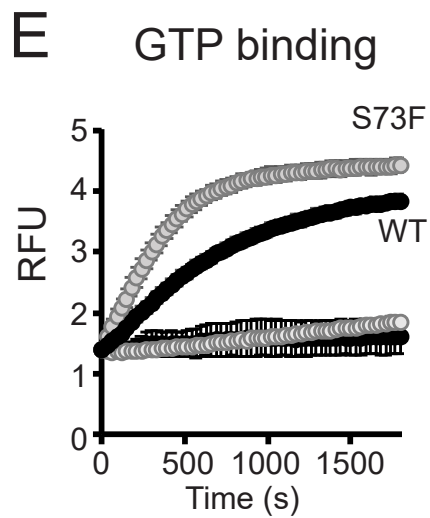
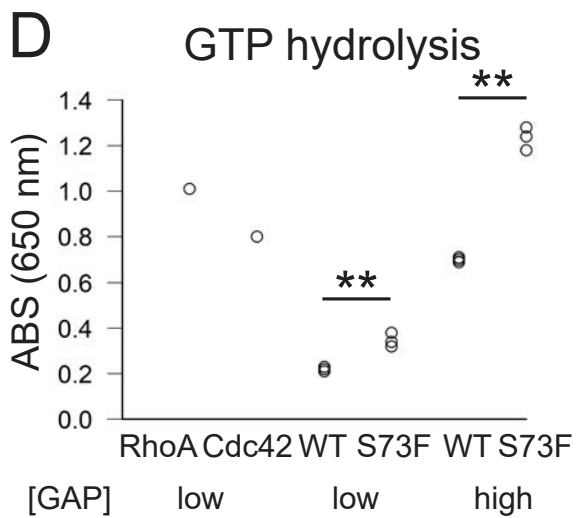
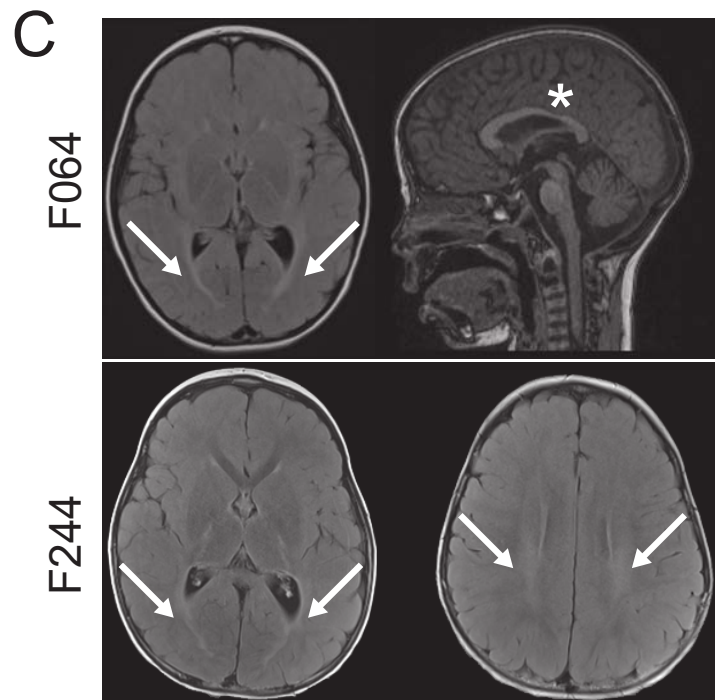
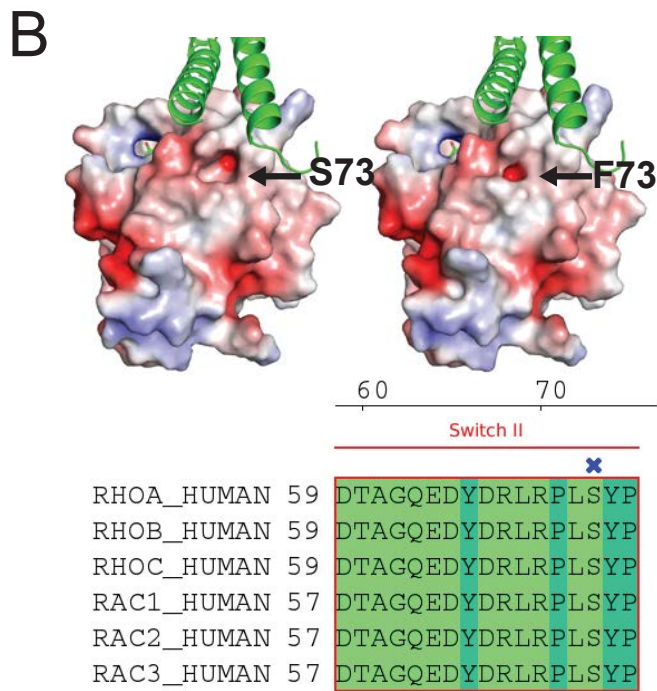
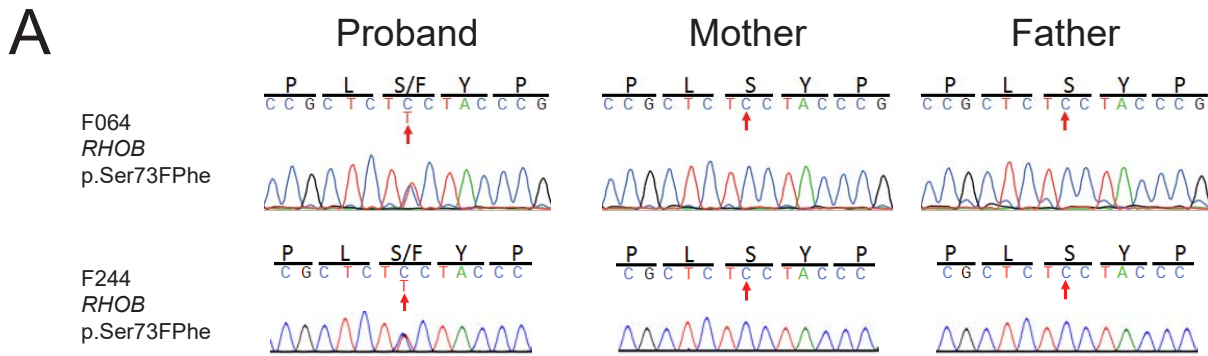
1176  
1177



1178 **METHODS-ONLY REFERENCES**

- 1179
- 1180 89. van Eyk, C.L. *et al.* Targeted resequencing identifies genes with recurrent  
1181 variation in cerebral palsy. *NPJ Genom. Med* **4**, 27 (2019).
- 1182 90. Miller, S.P., Shevell, M.I., Patenaude, Y. & O’Gorman, A.M. Neuromotor  
1183 spectrum of periventricular leukomalacia in children born at term. *Pediatr. Neurol.*  
1184 **23**, 155-159 (2000).
- 1185 91. Li, H. & Durbin, R. Fast and accurate long-read alignment with Burrows-Wheeler  
1186 transform. *Bioinformatics* **26**, 589-595 (2010).
- 1187 92. Wang, K., Li, M. & Hakonarson, H. ANNOVAR: functional annotation of genetic  
1188 variants from high-throughput sequencing data. *Nucleic Acids Res.* **38**, e164  
1189 (2010).
- 1190 93. Lek, M. *et al.* Analysis of protein-coding genetic variation in 60,706 humans.  
1191 *Nature* **536**, 285-291 (2016).
- 1192 94. 1000 Genomes Project Consortium *et al.* A global reference for human genetic  
1193 variation. *Nature* **526**, 68-74 (2015).
- 1194 95. Ware, J.S., Samocha, K.E., Homsy, J. & Daly, M.J. Interpreting de novo Variation  
1195 in Human Disease Using denovolyzeR. *Curr. Protoc. Hum. Genet.* **87**, 7 25 1-15  
1196 (2015).
- 1197 96. Homsy, J. *et al.* De novo mutations in congenital heart disease with  
1198 neurodevelopmental and other congenital anomalies. *Science* **350**, 1262-1266  
1199 (2015).
- 1200 97. Huang da, W., Sherman, B.T. & Lempicki, R.A. Bioinformatics enrichment tools:  
1201 paths toward the comprehensive functional analysis of large gene lists. *Nucleic*  
1202 *Acids Res.* **37**, 1-13 (2009).
- 1203 98. Mi, H., Muruganujan, A., Ebert, D., Huang, X. & Thomas, P.D. PANTHER version  
1204 14: more genomes, a new PANTHER GO-slim and improvements in enrichment  
1205 analysis tools. *Nucleic Acids Res.* **47**, D419-D426 (2019).
- 1206 99. Subramanian, A. *et al.* Gene set enrichment analysis: a knowledge-based  
1207 approach for interpreting genome-wide expression profiles. *Proc. Natl. Acad. Sci.*  
1208 *USA* **102**, 15545-15550 (2005).

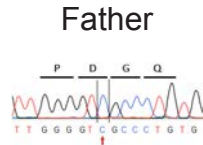
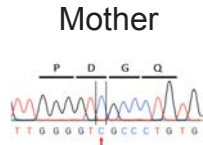
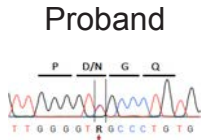
1209  
1210  
1211  
1212  
1213  
1214  
1215  
1216  
1217  
1218  
1219  
1220  
1221  
1222



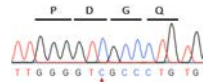
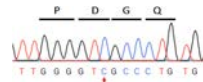
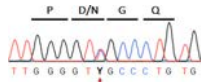
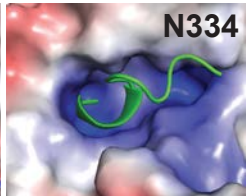
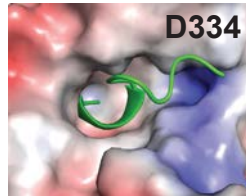
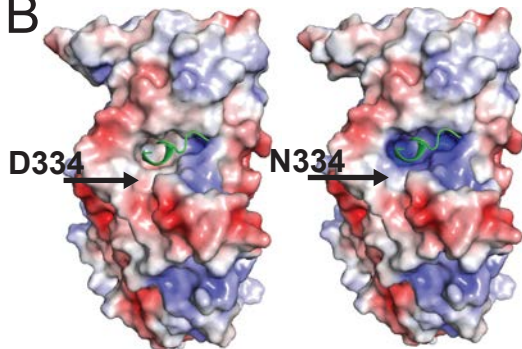
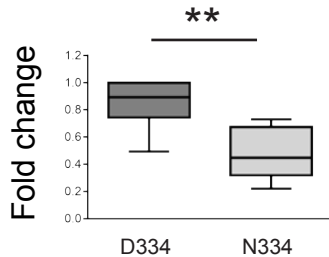
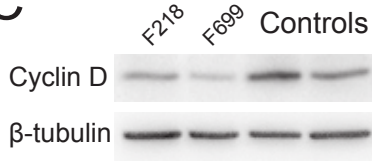


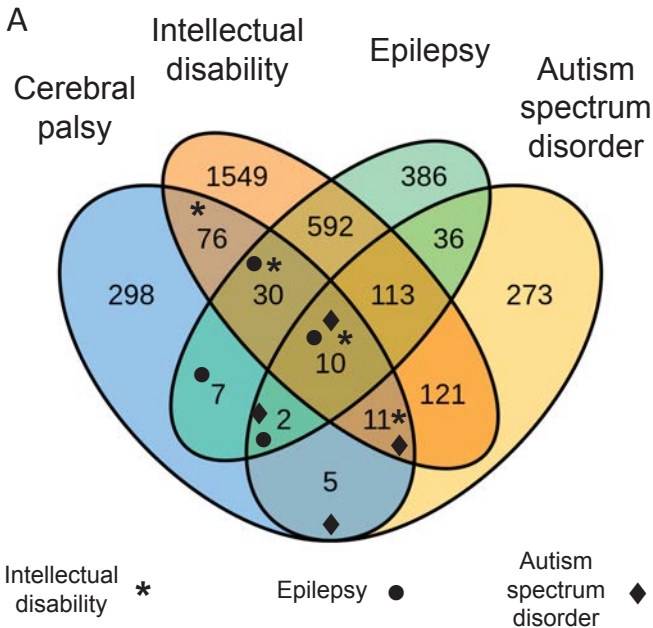
**A**

F218  
*FBXO31*  
 p.Asp334Asn



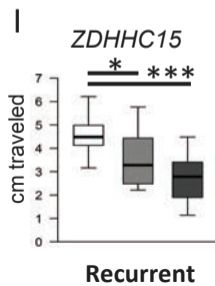
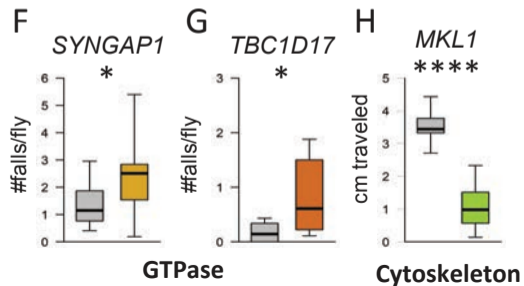
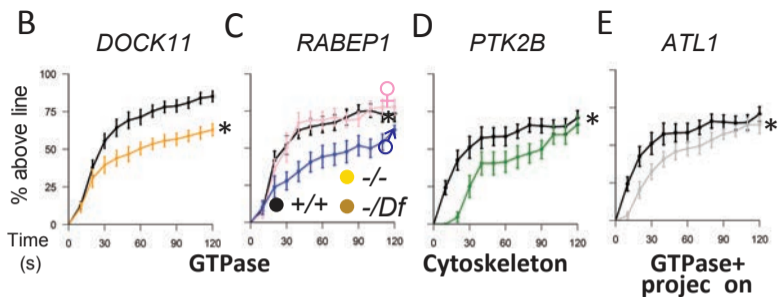
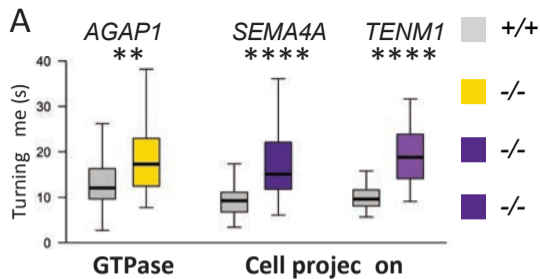
F699  
*FBXO31*  
 p.Asp334Asn

**B****C**



**B**

Disease	Genes in DisGeNET	CP candidate genes overlapping with DisGeNET	P-value
ASD	571	28	◆ $1.20 \times 10^{-5}$
ID	2502	127	* $2.56 \times 10^{-16}$
Epilepsy	1176	49	● 0.00016
Alzheimer's	1981	47	0.617



**J**

	Locomotor defect	No defect
Current study	16	6
Annotated	432	13499
Enrichment	23.4	
P-value	$2.2 \times 10^{-16}$	